

University of Nebraska - Lincoln

DigitalCommons@University of Nebraska - Lincoln

Center for Plant Science Innovation: Faculty and
Staff Publications

Plant Science Innovation, Center for

4-18-2024

Post-Translational Regulation of a Bidomain Glycerol-3-Phosphate Dehydrogenase Catalyzing Glycerol Synthesis under Salinity Stress in *Chlamydomonas reinhardtii*

Itzela Cruz-Powell

Binita Subedi

Yeongho Kim

Daniela Morales-Sánchez

Heriberto D. Cerutti

Follow this and additional works at: <https://digitalcommons.unl.edu/plantscifacpub>



Part of the [Plant Biology Commons](#), [Plant Breeding and Genetics Commons](#), and the [Plant Pathology Commons](#)

This Article is brought to you for free and open access by the Plant Science Innovation, Center for at DigitalCommons@University of Nebraska - Lincoln. It has been accepted for inclusion in Center for Plant Science Innovation: Faculty and Staff Publications by an authorized administrator of DigitalCommons@University of Nebraska - Lincoln.

Article

Post-Translational Regulation of a Bidomain Glycerol-3-Phosphate Dehydrogenase Catalyzing Glycerol Synthesis under Salinity Stress in *Chlamydomonas reinhardtii*

Itzela Cruz-Powell, Binita Subedi, Yeongho Kim , Daniela Morales-Sánchez  and Heriberto Cerutti * 

School of Biological Sciences and Center for Plant Science Innovation, University of Nebraska-Lincoln, Lincoln, NE 68588, USA; i.cruz@outlook.com (I.C.-P.); bsubedi2@huskers.unl.edu (B.S.); yeongho.kim@yale.edu (Y.K.); daniela.morales@ibt.unam.mx (D.M.-S.)

* Correspondence: hcerutti1@unl.edu

Abstract: Core chlorophytes possess glycerol-3-phosphate dehydrogenases (GPDs) with an unusual bidomain structure, consisting of a glycerol-3-phosphate phosphatase (GPP) domain fused to canonical GPD domains. These plastid-localized enzymes have been implicated in stress responses, being required for the synthesis of glycerol under high salinity and triacylglycerols under nutrient deprivation. However, their regulation under varying environmental conditions is poorly understood. *C. reinhardtii* transgenic strains expressing constitutively bidomain GPD2 did not accumulate glycerol or triacylglycerols in the absence of any environmental stress. Although the glycerol contents of both wild type and transgenic strains increased significantly upon exposure to high salinity, cycloheximide, an inhibitor of cytoplasmic protein synthesis, abolished this response in the wild type. In contrast, GPD2 transgenic strains were still capable of glycerol accumulation when cultured in medium containing cycloheximide and NaCl. Thus, the pre-existing GPD2 protein appears to become activated for glycerol synthesis upon salt stress. Interestingly, staurosporine, a non-specific inhibitor of protein kinases, prevented this post-translational GPD2 protein activation. Structural modeling analyses suggested that substantial conformational rearrangements, possibly triggered by high salinity, may characterize an active GPD2 GPP domain. Understanding this mechanism(s) may provide insights into the rapid acclimation responses of microalgae to osmotic/salinity stress.

Keywords: osmotic stress; glycerol-3-phosphate phosphatase; phosphorylation; kinase inhibition; chloroplast



Citation: Cruz-Powell, I.; Subedi, B.; Kim, Y.; Morales-Sánchez, D.; Cerutti, H. Post-Translational Regulation of a Bidomain Glycerol-3-Phosphate Dehydrogenase Catalyzing Glycerol Synthesis under Salinity Stress in *Chlamydomonas reinhardtii*. *Phycology* **2024**, *4*, 213–234. <https://doi.org/10.3390/phycolgy4020012>

Academic Editor: Koji Mikami

Received: 15 March 2024

Revised: 15 April 2024

Accepted: 17 April 2024

Published: 18 April 2024



Copyright: © 2024 by the authors. Licensee MDPI, Basel, Switzerland. This article is an open access article distributed under the terms and conditions of the Creative Commons Attribution (CC BY) license (<https://creativecommons.org/licenses/by/4.0/>).

1. Introduction

Microalgae can live in a variety of environments, due to their ability to withstand changing and, sometimes, extreme conditions. For instance, unicellular green algae from the genus *Chlamydomonas* have been found in soil, freshwater, oceans, deserts, and even in snow or sea ice, where they can face substantial variations in salinity [1–6]. The genus *Chlamydomonas* currently consists of several hundred species, but it is highly polyphyletic [7,8]. *Chlamydomonas reinhardtii* is a well-established model system for examining photosynthesis, physiology, metabolism and the structure and function of flagella [3,4,9]. However, most contemporary laboratory strains of *C. reinhardtii*, including those used in the work described here, are derived from a single zygote isolated from a potato field in Massachusetts in 1945 [3,4].

Salinity is one of the key environmental factors affecting the growth and distribution of microalgae. Organisms exposed to salt stress have to cope with ionic and osmotic imbalances, as well as toxicity effects, such as oxidative damage [5,6,10,11]. Under these conditions, many microorganisms counteract dehydration through the intracellular accumulation of one or more compatible solutes, small organic molecules characterized by a neutral charge and low toxicity at high concentrations [5,6,11]. Glycerol is a common

osmolyte synthesized by several yeast species and microalgae, including *C. reinhardtii* and *Dunaliella* spp. [1,2,5,6,10–17]. This compatible solute contributes to the osmotic balance of cells and the maintenance of enzyme activities under conditions of cell shrinkage, molecular crowding and low water activity [10–12,14].

Glycerol is generally synthesized in a two-step pathway from the glycolytic intermediate dihydroxyacetone phosphate (DHAP) (Figure 1), although an alternative pathway via dihydroxyacetone has been proposed in some species [6,10,11,14,15]. In the first step, NAD(P)⁺-dependent glycerol-3-phosphate dehydrogenases (GPDs) catalyze the reduction of DHAP to glycerol-3-phosphate (G3P). In the second step, G3P is dephosphorylated to glycerol by glycerol-3-phosphate phosphatases (GPPs). Microalgae in the Chlorophyceae and Trebouxiophyceae classes encode GPDs with an unusual bidomain structure, consisting of a phosphoserine phosphatase-like domain fused to canonical glycerol-3-phosphate dehydrogenase domains [5,15,17–19]. Recent work has demonstrated that two of these bidomain enzymes, *C. reinhardtii* GPD2 [15] and *D. salina* osmoregulated GPDH [17], can convert DHAP directly to glycerol, indicating that the phosphoserine phosphatase-like domain actually functions as a GPP.

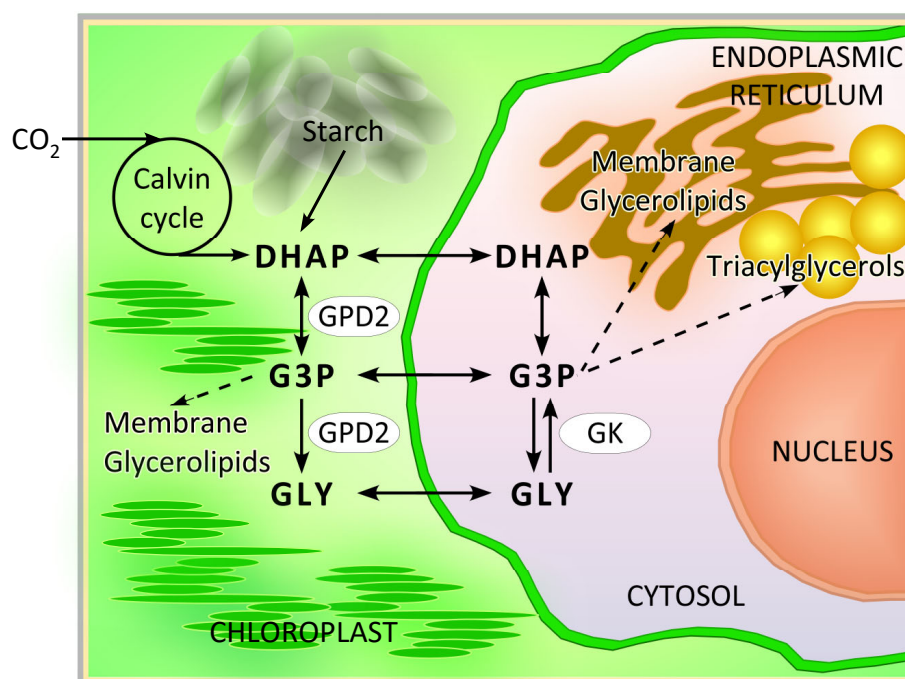


Figure 1. Simplified pathway of glycerol metabolism in *C. reinhardtii* and connections to membrane glycerolipid and triacylglycerol synthesis. For additional details, see Morales-Sánchez et al. [15]. Metabolites: DHAP, dihydroxyacetone phosphate; G3P, glycerol-3-phosphate; Gly, glycerol. Enzymes: GPD2, bidomain NAD(P)⁺-dependent glycerol-3-phosphate dehydrogenase isoform 2; GK, glycerol kinase.

C. reinhardtii possesses five NAD(P)⁺-dependent GPD homologs and the genes encoding two bidomain isoforms (i.e., GPD2 and GPD3), in particular *GPD2*, were substantially upregulated upon exposure of cells to NaCl [15,19,20]. By using pulse labeling with ¹³C-arginine in an auxotrophic strain, an increase in the rate of synthesis of the GPD2 protein (ID 146945) was also observed in cells exposed to NaCl [21]. Moreover, consistent with enhanced activity of the corresponding enzyme(s), the acclimation of *C. reinhardtii* to hyperosmotic stress involved the rapid accumulation of glycerol, as well as several other sugars [13,16,22]. However, various proteomic experiments examining cells subjected to osmotic/salt stress failed to detect any bidomain GPD protein [16,23]. Other chlorophytes also showed increased expression of genes encoding bidomain GPDs in response to osmotic/salinity stress. In a psychrophilic species of *Chlamydomonas* (UWO 241), a bidomain

GPD gene was strongly upregulated by NaCl exposure, correlating with an increase in intracellular glycerol concentration [5]. In the halotolerant alga *Dunaliella salina*, bidomain GPDs are encoded by a small multigene family and *DsaGPD2* and *DsaGPD4* exhibited substantial induction upon high salt stress [18,24]. In *Dunaliella viridis*, two bidomain GPD encoding genes were also transiently induced in response to hypersalinity shock [25]. However, at least in *Dunaliella tertiolecta*, even though the intracellular glycerol concentration increased substantially after salt stress, no significant changes in the abundance of bidomain GPD proteins were detected in proteomic analyses [26].

The bidomain GPDs encoded by genes upregulated under salinity stress in *C. reinhardtii* and *D. salina* localize to the chloroplast [15,17], suggesting that they are key components of a distinctive plastid pathway for fast glycerol synthesis during acclimation to hyperosmotic stress. However, in *C. reinhardtii*, *GPD2* and *GPD3* transcript abundance also increased substantially under nitrogen- or phosphorus-deprivation, conditions that trigger the accumulation of carbon storage compounds such as triacylglycerols (TAGs) [15,20,27,28]. In fact, the G3P produced by GPD enzymes is also an intermediate in lipid biosynthesis (Figure 1), forming the backbone of membrane glycerolipids and TAGs [6,15,20], and it may act as a bridge for carbon transfer between carbohydrate and lipid metabolism [29]. Furthermore, the knockdown of *C. reinhardtii* *GPD2* expression by RNA interference demonstrated its requirement for both glycerol accumulation under NaCl stress [15] and TAG accumulation under N- or P-deprivation [15,20].

Thus, changes in the expression and/or the activity of bidomain GPDs seem to be an important part of the response of diverse microalgae to environmental stresses such as hypersalinity or nutrient deprivation. However, the regulatory mechanism(s) is poorly understood, and some observations appear to be incongruous. For instance, several chlorophytes significantly upregulate bidomain GPD gene expression in response to salt stress, but the corresponding proteins are not detected or do not change in abundance. Discerning this regulatory mechanism(s) may enhance our understanding of algal stress responses, but it may also have biotechnological implications for the sustainable production of glycerol through direct CO₂ capture. Interestingly, for membrane glycerolipid and TAG synthesis, the production of G3P (rather than glycerol) as the final product of bidomain GPD activity would be energetically favored. Otherwise, glycerol would need to be converted back to G3P, with ATP expenditure, by a glycerol kinase (Figure 1). This reasoning prompted us to propose that the canonical GPD domains (with reductase activity) and the GPP domain (with phosphatase activity) of bidomain GPDs may be regulated independently by a post-translational mechanism(s), allowing these enzymes to synthesize primarily G3P or glycerol depending on environmental conditions or metabolic demands [15]. In the present study, we tested this hypothesis by examining the regulation of transgenic *C. reinhardtii* *GPD2* in cells exposed to salinity stress.

2. Materials and Methods

2.1. Strains and Culture Conditions

C. reinhardtii CC-124 (wild type) and transgenic *GPD2* overexpression strains (described below) were used in all reported experiments. Unless specified otherwise, 100 mL cultures (in 500 mL flasks) were incubated on an orbital shaker under continuous illumination at 25 °C and ambient level of CO₂ [15,30]. Strains were pre-cultured to the middle of the logarithmic phase ($\sim 3 \times 10^6$ cells mL⁻¹) in minimal HS medium [31]. As previously described [15], cells were then collected by centrifugation, washed twice, and resuspended in either HS medium, HS medium containing 100 mM NaCl (HS+NaCl), or HS medium lacking nitrogen (HS-N) at a density of $\sim 2.0 \times 10^6$ cells mL⁻¹. Cells were next cultured under photoautotrophic conditions during 6 h for the high salinity experiments or during 48 h for the nitrogen deprivation analyses. At the end of the experimental period, cells were harvested by centrifugation at $2000 \times g$ for 5 min and the pellets were frozen in liquid nitrogen and stored at -70 °C for further analyses. For experiments examining glycerol accumulation under light or dark conditions, cells in the middle of the logarithmic phase

($\sim 3 \times 10^6$ cells mL⁻¹), pre-grown in either HS minimal medium or Tris-Acetate-Phosphate (TAP) medium [32], were cultured in the same medium for three days in complete darkness. After this pre-treatment, cells were incubated for an additional 6 h under continuous light or dark in HS (or TAP) medium (as controls) or in HS (or TAP) medium containing 100 mM NaCl.

2.2. Construction of the PSAD:GPD2:PSAD Transgene and Generation of Transgenic Strains

The *GPD2* (Cre01.g053000) coding sequence was amplified by PCR from plasmid pIVEX-GPD2 [15] by using primers GPD2_F (5'-GGTACCATGATGCTGTCAGGCCGCACCTGC) and GPD2-AcV5_R (5'-GAATTCttagctccagccgctggcgtctctccagctCACGCTGTTGCTGGCAGC). The reverse primer inserted the sequence of the AcV5 tag [33] at the 3' end of the *GPD2* CDS. This PCR product was cloned into pSTBlue1 (Novagen, Madison, WI, USA), verified by sequencing, and then excised as a GPD2-AcV5 fragment by successive digestion with *KpnI*, blunting by T4 polymerase treatment, and digestion with *EcoRI*. Simultaneously, plasmid NE589, derived from pGenD containing *PSAD* regulatory sequences [34], was digested with *NcoI*, blunted by T4 polymerase treatment, and digested with *EcoRI*. The linearized NE589 plasmid and the GPD2-AcV5 fragment were then ligated, and this new construct was digested with *NsiI*, blunted by T4 polymerase treatment, and self-ligated to generate the *PSAD:GPD2:PSAD* transgene in the proper reading frame within plasmid NE589. This transgene was excised by digestion with *KpnI* and *XbaI* and inserted by blunt-end cloning, after treatment with T4 DNA polymerase, into the *EcoRI* site of plasmid pSP124S, which contains the Zeocin-resistance *Ble^r* selectable marker [35]. The final plasmid was transformed into CC-124 by electroporation, as previously described [36], and colonies were selected on TAP-agar plates containing 16 μ g mL⁻¹ zeocin (Invitrogen, Carlsbad, CA, USA, R25001). Expression of the *GPD2* recombinant protein was corroborated in several independent transgenic strains by immunoblotting with an anti-AcV5 monoclonal antibody (please see below).

2.3. Reverse Transcriptase (RT-) and Quantitative Real Time (qRT-) PCR Assays

Total RNA extraction, reverse transcription, and standard PCR amplification were performed following previously described procedures [15]. Before qRT-PCR assays, primers were confirmed to amplify a single-sized product by end-point PCR and examination by agarose gel electrophoresis. DNA fragments were then amplified and quantified with the RT² SYBR Green/Fluorescein qPCR Mastermix (Qiagen, Hilden, Germany, 330519), using the CFX96 Touch™ Real-Time PCR Detection System (Bio-Rad, Hercules, CA, USA). The qRT-PCR analyses were based on three biological replicates and three technical replicates. *ACT1*, encoding actin, was used as a reference gene to normalize gene expression levels. The primers used for *GPD2* amplification anneal to both the endogenous (wild type) and the transgenic transcripts. The primer sequences were as follows: for *GPD2* (Cre01.g053000) GPD2-RT-F1 5'-GCAAGTACCCGCTGTTCAC-3' and GPD2-RT-R1 5'-GCACAATATCCTCCTCGACGT-3'; for *HSF1* (Cre09.g387150, *HEAT SHOCK FACTOR 1*) HSF1F 5'-AACATCGTCTCATGGGGTGC-3' and HSF1R 5'-TCCATAGGTGTTGAGCTGGC-3'; and for *ACT1* (Cre13.g603700), ACT-cod-F 5'-GACATCCGCAAGGACCTCTAC-3' and ACT-cod-R 5'-GATCCACATTTGCTGGAAGGT-3'.

2.4. Glycerol and Non-Polar Lipid Analyses

Glycerol content was determined as previously described [15]. Briefly, *C. reinhardtii* cells were collected by centrifugation, washed in an isotonic solution, and the pellets frozen in liquid nitrogen and stored at -70 °C until use. Pellets were resuspended in deionized water, briefly vortexed, and boiled for 10 min to release the glycerol from cells. Cell debris was pelleted by centrifugation at $2000 \times g$ for 5 min and the supernatant was used for measuring glycerol amounts with the free glycerol reagent (Sigma, St. Louis, MO, USA, F6428). To assess the content of non-polar lipids, cells were stained with the lipophilic fluorophore Nile Red, as previously described [37]. About 100 μ L of cells were transferred

to a multi-well plate and mixed with 100 μL of HS medium. Then, Nile Red (Sigma, 72485) was added to a final concentration of 1 $\mu\text{g mL}^{-1}$ and fluorescence (excitation at 488 nm; emission at 565 nm) was measured in a multi-well plate reader (Synergy H1, Biotek, Winooski, VT, USA). Nile Red fluorescence was finally normalized to cell density (determined as absorbance at 750 nm) and expressed in arbitrary units.

2.5. Immunoblot Analyses

Approximately 5×10^7 cells were pelleted by centrifugation and resuspended in 50 μL of SDS-gel running buffer [38]. Samples were heated at 95 $^{\circ}\text{C}$ for 8 min and 5- μL aliquots of whole-cell protein extracts were separated by 10% SDS-PAGE and electrophoretically transferred to a nitrocellulose membrane (Cytiva, Marlborough, MA, USA, Amersham Protran 10600003) [38]. The membrane was then blocked with 7% nonfat dry milk in TBS-T buffer (Tris-Buffered Saline containing 0.1% Tween-20) and incubated overnight at 4 $^{\circ}\text{C}$ with a 1:5000 dilution, in the same buffer, of a mouse anti-AcV5 antibody (Thermo Fisher Scientific, Waltham, MA, USA, 14-6995). After washing three times (10 min each) with TBS-T buffer, the nitrocellulose membrane was blocked again with 7% nonfat dry milk in TBS-T and incubated at 4 $^{\circ}\text{C}$ for 2 h with a goat anti-mouse IgG conjugated to horseradish peroxidase (Sigma, A2304) in the same buffer. Finally, the membrane was washed three times (10 min each) in TBS-T buffer and the signal was detected with Immobilon Chemiluminescent HRP substrate (Millipore, Burlington, MA, USA, WBKLS0500) and autoradiography (Cytiva, Marlborough, MA, USA, Amersham Hyperfilm MP 28906845). To evaluate the loading of the lanes, we used a modification-insensitive polyclonal anti-histone H3 antibody (Abcam, Cambridge, United Kingdom, ab1791) at a 1:5000 dilution.

2.6. Treatments with Pharmacological Agents

Unless noted otherwise, stock solutions of the chemicals were prepared in dimethyl sulfoxide (DMSO), added to cell cultures 1 h before the start of the experimental treatments (i.e., before exposing the cells to 100 mM NaCl or N-deprivation), and left in the medium for the duration of the experiments (usually, 6 h for NaCl stress and 48 h for N-deprivation). The compounds were used at the following final concentrations: cycloheximide 150 $\mu\text{g mL}^{-1}$ (Sigma, 239763-M); N-acetyl-L-cysteine 5 mM (Sigma, A7250); spectinomycin 100 $\mu\text{g mL}^{-1}$ (Sigma, 567570); staurosporine 1 μM (Sigma, 569397); and Torin1 1 μM (Cayman Chemicals, Ann Arbor, MI, USA, 10997). Unlike the other compounds, okadaic acid (Sigma, 495604) was added to the cultures 24 h before the start of the experimental treatments at a final concentration of 10 nM (or as indicated in the figures). The stock solution of cycloheximide was prepared in ethanol and that of spectinomycin in water.

2.7. Proteomic Analyses

Transgenic AcV5-tagged GPD2 protein was purified from cells in the middle of the logarithmic phase maintained in HS medium (HS) or exposed to 100 mM NaCl for 6 h (HS+NaCl) by using a previously described protocol [39] with some modifications. Briefly, for each treatment, $\sim 10^{10}$ cells were resuspended in 10 mL of lysis buffer [20 mM Tris-HCl (pH 7.0), 150 mM NaCl, 0.1 mM EDTA, 2.0 mM $\text{Mg}(\text{CH}_3\text{COO})_2$, 2.0 mM Benzamidine, 0.2 mM phenylmethanesulfonyl fluoride (PMSF), and 10% glycerol] containing 5 $\mu\text{L mL}^{-1}$ plant protease inhibitor cocktail (Sigma, P9599), and phosphatase inhibitor cocktail (Sigma, PhosSTOP, PHOSS-RO; 1 tablet in 10 mL of buffer). Cells were broken by two passages through a French press at ~ 5000 psi and the lysate was clarified by centrifugation at $16,000 \times g$ for 30 min at 4 $^{\circ}\text{C}$. The extract was centrifuged again at $80,000 \times g$ for 90 min and the supernatant was then incubated at 4 $^{\circ}\text{C}$ with 20 μg of a mouse anti-AcV5 antibody (Thermo Fisher Scientific, 14-6995) for 1 h followed by overnight incubation with protein G-agarose beads (Sigma, P7700; ~ 200 μL of packed resin per 40 mL of original cell extract). The beads were collected by centrifugation ($5000 \times g$ for 5 min) and washed five times with wash buffer [20 mM Tris-HCl (pH 7.0), 300 mM NaCl, 0.1 mM EDTA, 2.0 mM $\text{Mg}(\text{CH}_3\text{COO})_2$, 2.0 mM Benzamidine, 0.2 mM PMSF, 0.1% Triton X-100, and 10% glycerol] containing

5 $\mu\text{L mL}^{-1}$ plant protease inhibitor cocktail and phosphatase inhibitor cocktail. Bead-bound proteins were then processed for liquid chromatography with tandem mass spectrometry (LC-MS/MS) analyses, as previously described [40]. Data were analyzed in Proteome Discoverer 2.2 software (Thermo Fisher Scientific) with MS Amanda 2.0 and SeQuest HT as search tools. The analytical pipeline has been described in detail before [40].

2.8. GPD2 Glycerol-3-Phosphate Phosphatase Domain Structure Predictions

Three-dimensional (3D) models of the *C. reinhardtii* GPD2 phosphatase domain were predicted in automated mode with Swiss Model [41], using as templates the crystal structures of *D. salina* dsGPDH 6iuy.1.a [17] or human phosphoserine phosphatase (hPSP) 6hyj.1.A. or 6hyj.2.A [42]. Evaluations of the models, analytic comparisons, and alternative visualizations and coloring were carried out within the Swiss Model workspace. We also examined an AlphaFold predicted 3D structure of *C. reinhardtii* GPD2 (AF-A0A0B5KTL4-F1), generated by a machine learning algorithm that combines knowledge from bioinformatics and physical Protein Data Bank approaches [43].

2.9. Statistical Data Analyses

Student's *t*-tests and one-way analyses of variance (ANOVA) were carried out using the "stats" package in the RStudio software AGPL v3 [44]. Based on the results, post hoc pairwise comparisons of group means were performed using the Tukey Honest Significant Difference (HSD), to identify the statistically different pairs ($p < 0.05$) in the data.

3. Results

3.1. *Chlamydomonas reinhardtii* GPD2 Transgenic Strains

Since we were primarily interested in examining the proposed post-translational regulation of bidomain GPD2, we decided to generate transgenic strains expressing this protein under the control of the *C. reinhardtii* *PSAD* regulatory sequences (i.e., promoter, 5' and 3' untranslated regions, and terminator) (Figure 2A). *PSAD* is a nuclear gene that encodes an abundant chloroplast-targeted protein, the subunit II of the Photosystem I reaction center [34]. Various transgenes constructed with *PSAD* regulatory sequences have been demonstrated to be expressed constitutively and at high levels in *C. reinhardtii* grown under continuous light [34]. Thus, *PSAD:GPD2:PSAD* transgenic strains would be expected to express the GPD2 protein in the absence of any environmental stress, when cultured in HS minimal medium under continuous light.

We generated several overexpression strains that showed substantial increases in *GPD2* transcript abundance relative to the wild type (CC-124) when grown in HS medium (Figure 2B, OX-9, OX-12, and OX-30). However, when cells were subject to salinity stress, the upregulated *GPD2* transcript levels were similar in the wild type and overexpression strains (Figure 2C). We next tested whether the overexpression strains could accumulate glycerol or non-polar lipids, such as TAGs, when cultured under normal environmental conditions in HS medium. Because of similar preliminary results with all overexpression strains, we focused our analyses on OX-12, showing intermediate *GPD2* transcript levels (Figure 2B), to avoid potential artifacts caused by excessive protein expression. Interestingly, the OX-12 strain, similarly to the wild type, only showed a significant increase in non-polar lipid content, as examined by staining cells with the lipophilic fluorophore Nile Red, when cells were subject to nitrogen deprivation (Figure 2D). Likewise, glycerol accumulation above background levels was only detected in cells cultured for 6 h in HS medium containing 100 mM NaCl (Figure 2E), and no significant differences in glycerol content were observed between OX-12 and the wild type. A previous study also generated *GPD2* overexpression strains, showing substantial increases in *GPD2* transcript levels, by using transgenes constructed with the tandem *HSP70A-RBCS2* promoter [20]. These strains were grown photoheterotrophically in TAP medium (containing acetate) with or without phosphorus limitation. However, none of the overexpression strains showed changes in glycerol accumulation, relative to the wild type, under the conditions tested. They did exhibit

increased total lipid content but only under low phosphorus stress, and the accumulated amounts were slightly lower than in the wild type cultured under the same conditions [20]. These combined results indicated that, despite significant increases in *GPD2* transcript levels in overexpression strains grown under normal environmental conditions, the contents of expected products of *GPD2* activity did not differ from the background levels detected in the wild type.

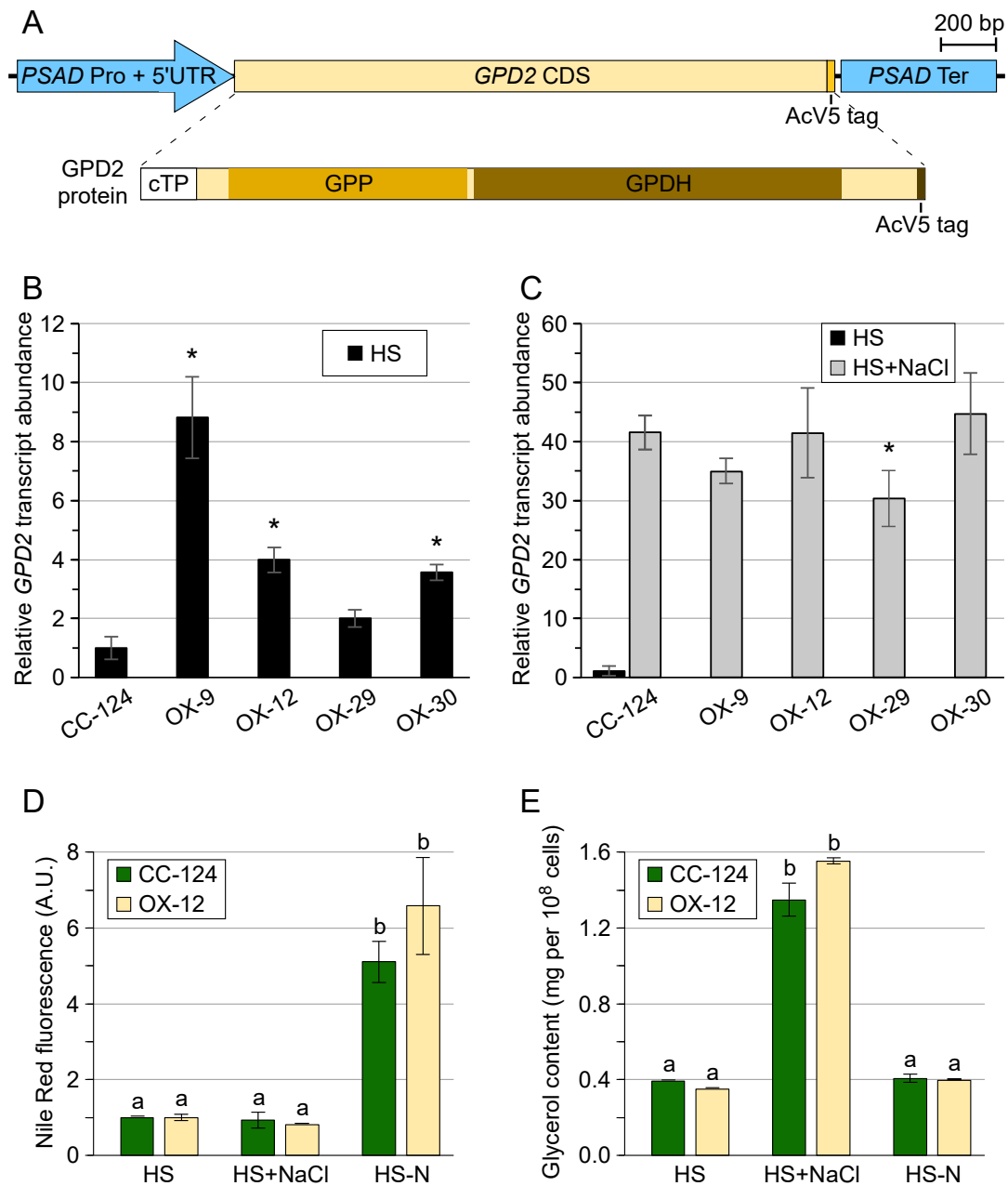


Figure 2. Characterization of *PSAD:GPD2:PSAD* transgenic strains. (A) Schematic diagram of the transgene designed to express the *GPD2* protein constitutively. cTP, chloroplast transit peptide; GPP, G3P phosphatase domain (related to phosphoserine phosphatase); GPDH, canonical G3P dehydrogenase domains; AcV5, epitope from the GP64 envelope fusion protein of *A. californica* multiple nuclear polyhedrosis virus; *PSAD* Pro, *PSAD* promoter; *PSAD* ter, 3'UTR and terminator from *PSAD*. (B) *GPD2* mRNA abundance in overexpression strains grown in minimal HS medium relative to the wild type (CC-124). Transcript expression was determined by qRT-PCR, and values

shown are the mean \pm standard deviation (SD) of three independent experiments ($n = 3$). Samples indicated with an asterisk are significantly different from the wild type ($p < 0.05$) in a two tailed Student's *t*-test. (C) *GPD2* mRNA abundance in overexpression strains grown in HS medium containing 100 mM NaCl (HS+NaCl) relative to CC-124 cultured under the same conditions. (D) Non-polar lipid accumulation in the wild type and overexpression strain OX-12 cultured under normal conditions (HS), high salinity (HS+NaCl) for 6 h, or nitrogen deprivation (HS-N) for 48 h. Non-polar lipid content was estimated by staining cells with the lipophilic fluorophore Nile Red. Fluorescence was normalized to cell density and expressed in arbitrary units (A.U.). Values indicate the mean \pm SD of three independent experiments ($n = 3$). Different lowercase letters indicate a significant difference among means (one way ANOVA with post hoc Tukey HSD test, $p < 0.05$). (E) Glycerol content in the wild type and overexpression strain OX-12 cultured as described above.

3.2. Transgenic *GPD2* Protein Abundance and Stability

We designed our transgenic construct with an epitope from the GP64 envelope fusion protein of *Autographa californica* multiple nuclear polyhedrosis virus (i.e., the AcV5 tag) [33] integrated at the carboxyl end of the *GPD2* protein (Figure 2A). This allowed us to monitor protein expression by immunoblotting with an anti-AcV5 monoclonal antibody. Transgenic *GPD2* protein was clearly detected in all overexpression strains when cells were grown in HS medium, in the absence of any environmental stress (Figures 3A and S1). Interestingly, when cells were cultured for 6 h in HS medium containing NaCl, the abundance of the transgenic *GPD2* protein was substantially reduced relative to that in cells maintained in HS medium (Figures 3A and S1). Similar results were observed when de novo cytoplasmic protein synthesis was inhibited by incubating cells with cycloheximide [45]. *GPD2* protein levels remained stable in cells cultured in HS medium containing cycloheximide and decreased markedly in cells cultured in HS medium containing both NaCl and cycloheximide (Figure 3A).

Despite the production of transgenic *GPD2* protein when cells were grown in HS medium, as already discussed, the glycerol content in overexpression strains did not differ from the background level detected in the wild type (Figure 2E). This suggested that transgenic *GPD2*, or at least its GPP domain, was inactive under normal environmental conditions. Thus, we designed an experiment to test whether the protein could be activated (or de-repressed) under salinity stress, coincidental with the observed changes in protein stability (Figure 3A). As already mentioned, the response of *C. reinhardtii* to hypersalinity involves the transcriptional upregulation of the *GPD2* gene, which is expressed at very low levels in the absence of environmental stresses (Figure 2C, wild type CC-124). Incubation of cells with cycloheximide is expected to abolish this response, since de novo cytoplasmic protein synthesis from the newly synthesized transcripts would be inhibited. In overexpression strains treated with cycloheximide before the NaCl stress, only pre-existent transgenic *GPD2* protein would be able to function. When untreated cells were cultured for 6 h in HS medium containing NaCl, glycerol content increased substantially and to similar levels in the wild type and OX-12 strains (Figure 3B, Ctrl). However, this response was completely abolished in the wild type strain when cells were incubated with cycloheximide for 1 h prior to the addition of NaCl (Figure 3B, Chx). In contrast, OX-12 cells treated with cycloheximide were still able to accumulate glycerol when stressed with NaCl (Figure 3B, Chx), although at a somewhat lower level than untreated cells. As an additional control, inhibition of organellar (particularly chloroplastic) protein synthesis with spectinomycin had no measurable effect on glycerol accumulation in any of the strains under the conditions tested (Figure 3B, Spec).

We also examined transgenic *GPD2* protein abundance when overexpression strains were subject to nitrogen deprivation for 48 h (Figure 3C). Again, when OX-12 cells were grown in minimal HS medium, despite the production of transgenic *GPD2* protein (Figure 3C), non-polar lipid content did not differ from that in the wild type (Figure 2D). Substantial accumulation of non-polar lipids, presumably TAGs, was only observed under nitrogen deprivation (Figure 2D). However, in contrast to the salinity stress experiment, the

abundance of transgenic GPD2 protein changed in a similar manner in cells cultured under nitrogen deprivation as in those maintained in HS medium for the same period (Figure 3C). Likewise, in cells incubated with cycloheximide to prevent de novo cytoplasmic protein synthesis, the abundance of transgenic GPD2 protein decreased similarly in cells subject to nitrogen deprivation as in those cultured in nutrient replete medium (Figure 3C, +Chx).

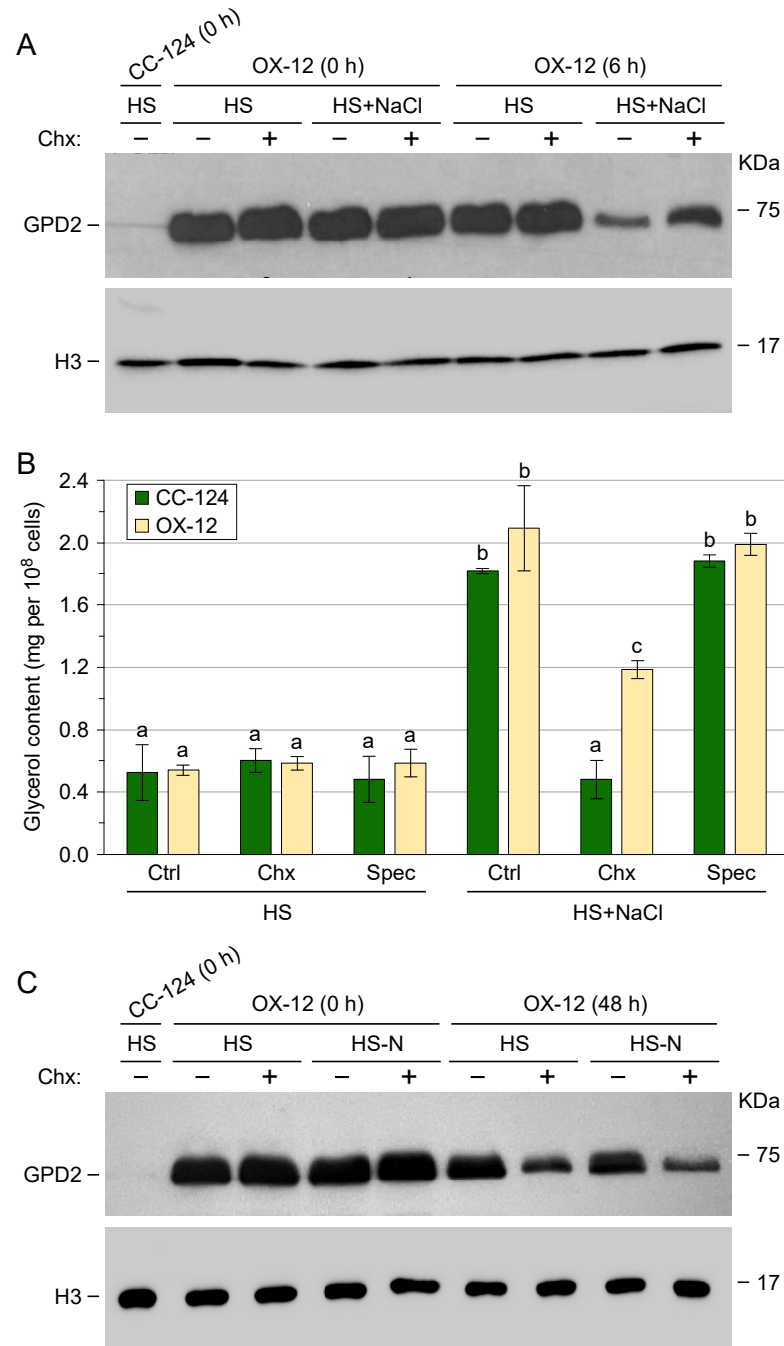


Figure 3. Analysis of GPD2 protein abundance and glycerol accumulation in overexpression strain OX-12 upon inhibition of cytoplasmic protein synthesis by cycloheximide. Cells were pre-incubated with cycloheximide for 1 h before the start of the experimental treatments. (A) Immunoblot analysis of transgenic GPD2 protein levels detected with an anti AcV5 antibody. OX-12 cells were cultured, for the indicated times, in minimal HS medium or HS medium containing 100 mM NaCl (HS+NaCl),

in the presence or absence of cycloheximide (Chx). Immunodetection of histone H3 was used as a control for equivalent loading of the lanes. The zero time (0 h) controls indicate that 1 h pre-incubation with cycloheximide did not alter, by itself, GPD2 protein abundance. (B) Glycerol content in the wild type and OX-12 strains grown for 6 h in HS medium or HS medium containing NaCl. Cells were cultured in the media alone (Ctrl) or with the addition of cycloheximide (Chx) or spectinomycin (Spec). Values indicate the mean \pm SD of three independent experiments ($n = 3$). Different lowercase letters indicate a significant difference among means (one way ANOVA with post hoc Tukey HSD test, $p < 0.05$). (C) Immunoblot analysis of transgenic GPD2 protein levels detected with an anti AcV5 antibody. OX-12 cells were cultured, for the indicated times, in minimal HS medium or HS medium lacking nitrogen (HS-N), in the presence or absence of cycloheximide (Chx). Immunodetection of histone H3 was used as a control for equivalent loading of the lanes.

The simplest interpretation of these observations is that the GPP domain of transgenic GPD2 is inactive when cells are grown in HS medium, under normal environmental conditions (please see Discussion). However, under salinity stress in the presence of cycloheximide, pre-existent GPD2 protein becomes activated (or de-repressed) to synthesize glycerol (Figure 3B, OX-12 HS+NaCl+Chx) but, at the same time, it is rapidly destabilized (Figure 3A, OX-12 HS+NaCl+Chx). Both effects might be related to conformational changes in the GPP domain ultimately triggered in response to NaCl stress (please see Discussion). In contrast, transgenic GPD2 protein stability was similar in cells cultured under nitrogen deprivation as in those maintained in nutrient replete medium (Figure 3C). Conceivably, only the canonical GPD domains of GPD2 might be active under these conditions (please see Discussion), where no increases in glycerol content were observed in the OX-12 strain. As previously reported for the wild type [15], *C. reinhardtii* overexpression strains accumulate appreciable amounts of non-polar lipids when subject to nitrogen deprivation (Figure 2D), suggesting that the G3P backbone is being produced. In nutrient replete medium, however, an expected increase in glycerol-3-phosphate dehydrogenase activity brought about by transgenic GPD2 might not alter the carbon flux directed to the synthesis of membrane glycerolipids (rather than storage TAGs) in rapidly growing cells. Indeed, when cells were grown in nutrient replete TAP medium, GPD2 overexpression strains only showed a significant increase in diglycerides relative to the wild type, but no differences in other lipid classes [20].

3.3. Control of Glycerol Accumulation under Salinity Stress

To explore the hypothesis that the GPP domain of GPD2 is activated (or de-repressed) under salinity stress, we examined glycerol accumulation in the wild type and OX-12 strains under a variety of treatments, aimed at identifying a plausible regulatory mechanism(s), including light exposure, scavengers of reactive oxygen species, and inhibitors of protein phosphatases or protein kinases. We first tested whether light was required for glycerol accumulation in *C. reinhardtii* under hypersalinity conditions. Cells, in the middle of the logarithmic phase, were cultured for three days in minimal HS medium under continuous darkness (to deplete them from stored starch), and then incubated for an additional 6 h under continuous light or dark in HS medium or HS medium containing 100 mM NaCl. Salinity stress triggered substantial glycerol accumulation in light-exposed cells, as before, but this response was abolished in the starch-depleted dark-incubated cells (Figure S2A). The same experiment was repeated with cells cultured in TAP medium, containing acetate as a source of carbon. In this case, dark-incubated cells also were capable of accumulating glycerol upon exposure to NaCl (Figure S2B), suggesting that acetate provided a carbon source for glycerol synthesis. Please also note the change in scale when comparing Figures S2A and S2B, indicating that cells cultured in acetate-containing medium accumulate much higher levels of glycerol than those cultured in minimal HS medium. These results are consistent with prior studies in several *Dunaliella* species indicating that light does not play a regulatory role in the synthesis of glycerol upon salinity/osmotic stress [12,46]; although photosynthesis does provide carbon skeletons and reducing power

for glycerol production. In *Dunaliella* spp., the products of both photosynthesis and starch breakdown contribute to glycerol synthesis in the light, whereas in the dark glycerol is mostly synthesized at the expense of starch degradation [12,46,47].

Besides its osmotic effects, high salinity can also stimulate the production of reactive oxygen species (ROS), leading to oxidative damage [6,16]. Thus, we also tested whether ROS signaling might be involved in triggering glycerol synthesis upon exposure of cells to NaCl. *N*-acetyl-L-cysteine (NAC) is a synthetic precursor of intracellular cysteine and glutathione, and it has antioxidant activity resulting from its free radical scavenging property, either directly via its thiol-disulfide exchange activity or secondarily via increasing glutathione levels in the cells [48]. NAC has been commonly used as a cell-permeable ROS scavenger in diverse organisms, including *C. reinhardtii* [49,50]. However, incubation of wild type and OX-12 cells with NAC did not affect the glycerol accumulation triggered by NaCl stress in any of the strains (Figure S2C).

The response to hyperosmotic stress and accumulation of glycerol in the yeast *Saccharomyces cerevisiae* involves several conserved signaling pathways, with the high osmolarity glycerol (HOG) pathway being the most prominent [11,16]. In this protein kinase cascade, the signal is often transmitted by reversible protein phosphorylation, modulating proteins' activity, localization and interactions with other proteins. Mitogen-activated protein kinases (MAPKs), related to yeast HOG1, have also been implicated in glycerol production under salt stress in *D. salina* and *D. tertiolecta* [51,52]. Moreover, proteomics analyses in *C. reinhardtii* subject to osmotic shock have suggested the involvement of stress-related kinases, such as MAPK6, and phosphatases in the initial cellular responses [16]. Thus, we tested whether protein phosphatase or protein kinase inhibitors might affect glycerol accumulation in our strains.

Okadaic acid (OA), a polyether fatty acid, is a strong inhibitor of protein phosphatases, specifically several serine/threonine phosphatases such as protein phosphatase 1 (PP1) and protein phosphatase 2A (PP2A) homologs [53,54]. OA was successfully used to inhibit PP1 phosphatases in *C. reinhardtii* [55], but short incubation times with the inhibitor failed to affect PP2A3 [56]. Based on *in vivo* studies, the amount of OA required to inhibit protein phosphatases varies, possibly because its uptake can be affected by pH, temperature, and exposure time [56]. Given these observations, we tested several OA concentrations and long, 24 h pre-incubation times in our experiments. Treatment of wild type *C. reinhardtii* with OA led to somewhat increased glycerol accumulation, relative to untreated cells, upon salt stress (Figure 4A). This was substantiated in a second experiment using the lowest effective concentration of OA (i.e., 10 nM) to minimize any non-specific effects (Figure 4B). However, under the same conditions, OX-12 cells incubated with OA did not show significantly higher glycerol accumulation than untreated cells (Figure 4B).

In metazoans and fungi, the target of rapamycin (TOR) protein kinase assembles into two complexes with distinct partners and independent functions [57,58]. In *S. cerevisiae*, the target of rapamycin complex 2 (TORC2) plays a role, independently from the HOG pathway, in a transient signaling response to hyperosmotic stress. High osmolarity prevents TORC2-mediated phosphorylation and activation of another kinase, YPK1, which in turn phosphorylates and inhibits one of the major glycerol-3-phosphate dehydrogenases, GPD1 [11]. Thus, under normal growth conditions, TORC2 has a repressive effect on GPD1 activity. By contrast, microalgae and other photosynthetic organisms only possess the target of rapamycin complex 1 (TORC1) [58], and the TOR kinase appears to have, at least transiently, a positive role in land plant responses to drought and osmotic stress [59–61].

In several studies in *C. reinhardtii* [57,62], Torin1 has been used to inhibit the TOR kinase with high specificity. Interestingly, when wild type *C. reinhardtii* was incubated with Torin1, glycerol accumulation triggered by NaCl stress was nearly entirely abolished (Figure 4C). In contrast, OX-12 cells treated with Torin1 were still able to synthesize glycerol when stressed with NaCl (Figure 4C). The effect of Torin1 on glycerol accumulation in the wild type and OX-12 strains was similar to that caused by the inhibition of cytoplasmic protein synthesis with cycloheximide (Figure 3B). Indeed, in cells exposed to NaCl, pre-

existent GPD2 protein was still able to synthesize glycerol in the presence of both Torin1 and cycloheximide (Figure 4D, OX-12 HS+NaCl+Tor1+Chx), suggesting that any post-translational regulatory mechanism(s) might be largely independent of TOR kinase activity. On the other hand, the TOR kinase appears to play a positive role in the accumulation of glycerol in response to salinity stress in wild type *C. reinhardtii*. However, further work will be necessary to assess its actual function, possibly affecting transcriptional and/or translational responses.

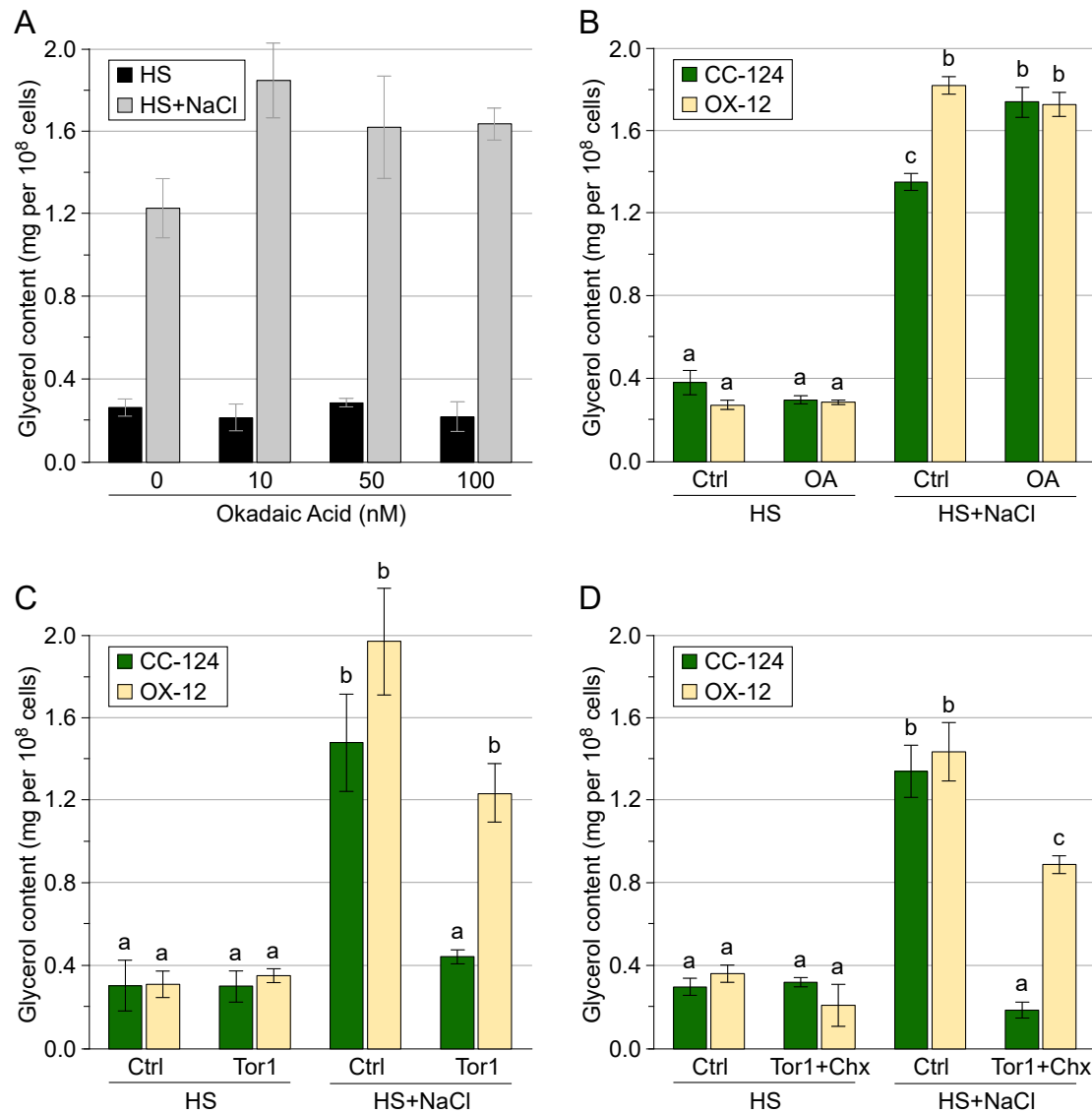


Figure 4. Effect of protein phosphatase and TOR kinase inhibitors on glycerol accumulation by the wild type and OX-12 strains. (A) Glycerol content in the wild type cultured in minimal HS medium or HS medium containing 100 mM NaCl (HS+NaCl) in the presence of the indicated concentrations of the protein phosphatase inhibitor okadaic acid. Values shown are the mean \pm SD of three independent experiments ($n = 3$). (B) Glycerol content in the wild type and OX-12 strains cultured in HS medium or HS medium containing NaCl, in the absence (Ctrl) or presence of 10 nM okadaic acid (OA). Values indicate the mean \pm SD of three independent experiments ($n = 3$). Different lowercase letters indicate a significant difference among means (one way ANOVA with post hoc Tukey HSD test, $p < 0.05$). (C) Glycerol content in the wild type and OX-12 strains cultured in HS medium or HS medium containing NaCl, in the absence (Ctrl) or presence of the TOR kinase inhibitor Torin 1 (Tor1). (D) Glycerol content in the wild type and OX-12 strains cultured in HS medium or HS medium containing NaCl, in the absence (Ctrl) or presence of both Torin 1 and cycloheximide (Tor1+Chx).

3.4. Post-Translational Regulation of Transgenic GPD2 Protein

To explore the possible involvement of other protein kinases in regulating glycerol accumulation under salinity stress, we also examined cells treated with the protein kinase inhibitor staurosporine. Due to its strong affinity for the ATP-binding site of kinases, staurosporine is a prototypical ATP competitor, but has very little selectivity [63]. To ensure that staurosporine was taken up by our *C. reinhardtii* strains, we first tested that it did inhibit, as previously reported [64], the transcriptional induction of *HEAT SHOCK FACTOR 1* (*HSF1*) after a heat shock treatment (Figure 5A). Of particular relevance to this study, the incubation of cells with staurosporine also completely abolished the glycerol accumulation triggered by salt stress in both wild type and OX-12 strains (Figure 5B). However, the abundance of transgenic GPD2 protein was still reduced in OX-12 cells incubated with staurosporine to an analogous extent as in untreated cells (Figure 5C, HS+NaCl). Similar results were observed when cells were treated with both staurosporine and the translation inhibitor cycloheximide (Figure 5D), indicating that staurosporine is blocking the NaCl-triggered activation (or de-repression) of pre-existent transgenic GPD2 protein for glycerol synthesis, but not its change in stability.

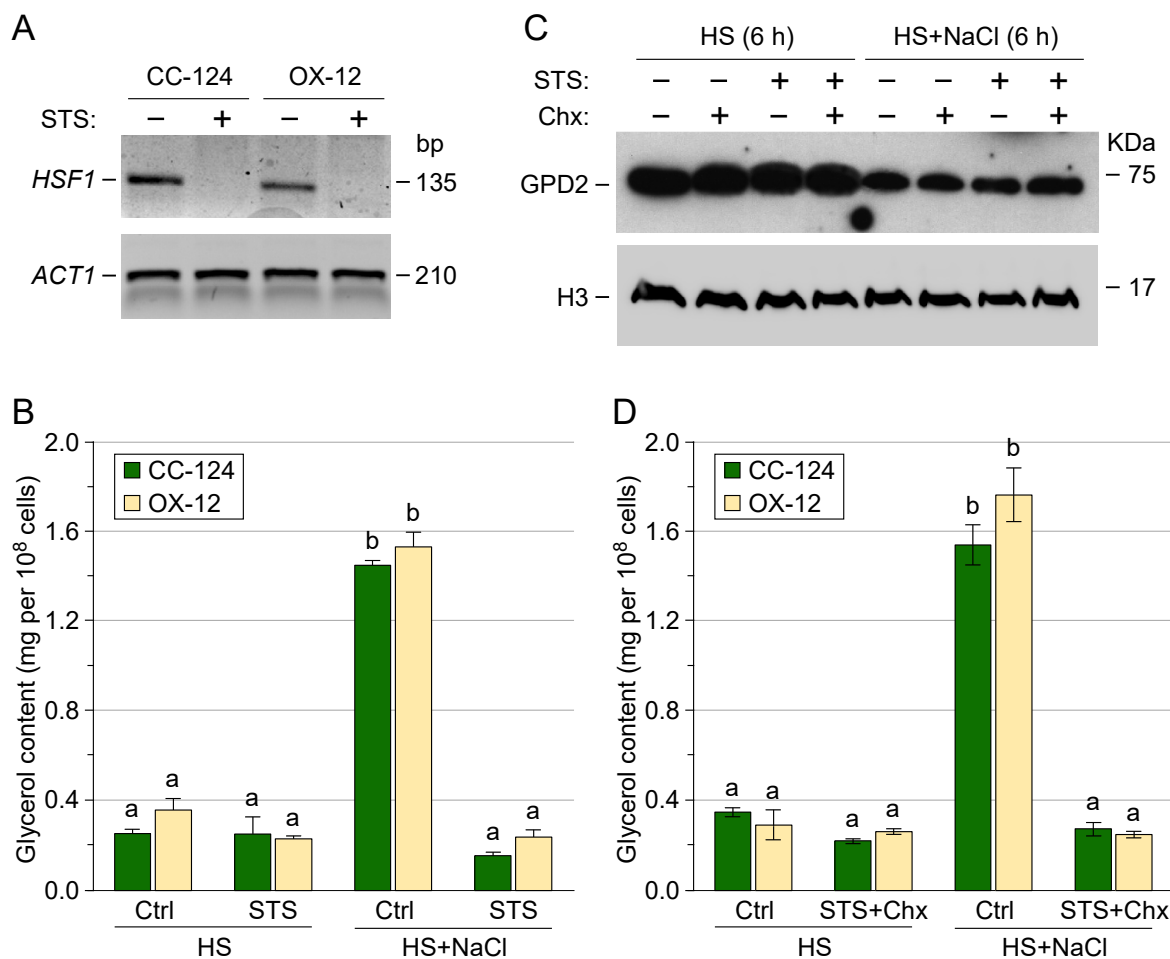


Figure 5. Effect of the non-specific protein kinase inhibitor staurosporine on glycerol accumulation by the wild type and OX-12 strains. (A) Semi-quantitative RT-PCR analysis of *HEAT SHOCK FACTOR 1* (*HSF1*) transcript abundance after exposing wild type and OX-12 cells to heat stress (40 °C for 20 min) in the absence or presence of staurosporine (STS). Amplification of the mRNA corresponding to *ACT1* was used as a control for equal amounts of input RNA and for the efficiency of the RT-PCRs. The panels show representative reverse images of agarose resolved PCR products stained with ethidium

bromide. (B) Glycerol content in the wild type and OX-12 strains cultured in HS medium or HS medium containing NaCl, in the absence (Ctrl) or presence of staurosporine (STS). Values indicate the mean \pm SD of three independent experiments ($n = 3$). Different lowercase letters indicate a significant difference among means (one way ANOVA with post hoc Tukey HSD test, $p < 0.05$). (C) Immunoblot analysis of transgenic GPD2 protein levels detected with an anti-AcV5 antibody. OX-12 cells were cultured, for the indicated times, in minimal HS medium or HS medium containing 100 mM NaCl, either in media alone or in the presence of cycloheximide (+Chx), staurosporine (+STS) or both cycloheximide and staurosporine (+Chx+STS). Immunodetection of histone H3 was used as a control for equivalent loading of the lanes. (D) Glycerol content in the wild type and OX-12 strains cultured in HS medium or HS medium containing NaCl, in the absence (Ctrl) or presence of both staurosporine and cycloheximide (STS+Chx).

These results suggested that a protein kinase(s) may play a role in the proposed post-translational regulation of transgenic GPD2 under salinity stress. However, it was unclear whether GPD2 itself and/or a protein(s) affecting GPD2 function might be the target of the putative kinase(s). We took advantage of the AcV5 epitope tag to partly enrich, by affinity purification, transgenic GPD2 protein from OX-12 cells cultured in HS medium or HS medium containing NaCl. These samples were examined by LC-MS/MS, as previously described [40], to identify differentially phosphorylated peptides. Unfortunately, GPD2 protein abundance was substantially reduced under salinity stress (as discussed above) making it difficult to purify enough protein to identify modified peptides with high confidence. In two independent experiments, a single phosphorylated peptide was detected exclusively in the NaCl-treated samples, albeit at only low to medium confidence (Figure S3A,B). The phosphorylated residue corresponded to Ser145 in the GPP domain of GPD2 (Figure S3C,D), and it is part of a conserved motif in bidomain GPD proteins from diverse microalgae (Figure S3B). However, in the predicted three-dimensional structure of the GPD2 GPP domain, generated either by homology modeling [41] using as a template the crystal structure of *D. salina* osmoregulated bidomain GPDH or by the AlphaFold algorithm [43], Ser145 is located far away from the Mg^{2+} -dependent catalytic center (Figure S3C,D). Thus, the functional relevance of Ser145 phosphorylation remains uncertain, although it could possibly be associated with conformational rearrangements of the GPP domain. Also, we cannot rule out that a protein kinase(s) inhibited by staurosporine might modify another protein which, in turn, affects GPD2 activity (via either interaction and/or post-translational modification).

3.5. Three-Dimensional Structure Prediction of the GPD2 GPP Domain

In order to explore potential conformational changes triggered by salinity stress, the GPP domain structure was predicted by homology modeling [41] using the crystal structures of *D. salina* osmoregulated bidomain GPDH (Figure 6A) or human phosphoserine phosphatase (PSP) (Figure 6B,E) as templates. As described for these two enzymes [17,42], the GPD2 GPP domain appears to consist of a Rossmann-fold-like motif with alternating α -helices and β -strands. This motif was modeled with a high degree of confidence, and corresponds to the putative catalytic core of the enzyme, including a Mg^{2+} atom (Figure 6A,B,E). Modeled with lower confidence was an α -helical cap domain (Figure 6A,B) that, in the haloacid dehalogenase (HAD) superfamily of enzymes, is used to shield the active site [42]. Detailed structural studies of the PSP family indicated that substantial conformational rearrangements of the active site (from open to closed conformation of the cap domain upon substrate binding) are required to catalyze the reaction [42,65]. An α -helix from the cap domain closes (and completes) the active site after phosphoserine binding, modeled for GPD2 GPP by using as template hPSP 6hyj.1.A (Figure 6B,D, "closed" cap domain). After catalysis, the α -helix unfolds into an open loop, allowing the products to leave the enzyme, modeled for GPD2 GPP by using as template hPSP 6hyj.2.A (Figure 6E, "open" cap domain). The "best fit" GPD2 GPP structure, modeled by using as template *D. salina* osmoregulated bidomain GPDH 6iuy.1.A (Figure 6A,C), predicts a cap

domain conformation somewhere in between the “closed” and “open” models. However, in the crystal structure of the *Dunaliella* enzyme (6iuy.1.A) electron density was missing for residues 248–256, and the folding of the cap domain was not completely solved [17]. Artificial intelligence-based structure prediction with the AlphaFold algorithm (43) resulted in a model (Figure S3D) with somewhat greater similarity to the “closed” cap domain. Nonetheless, these structural modeling analyses suggest that extensive conformational rearrangements may characterize an active GPD2 GPP domain.

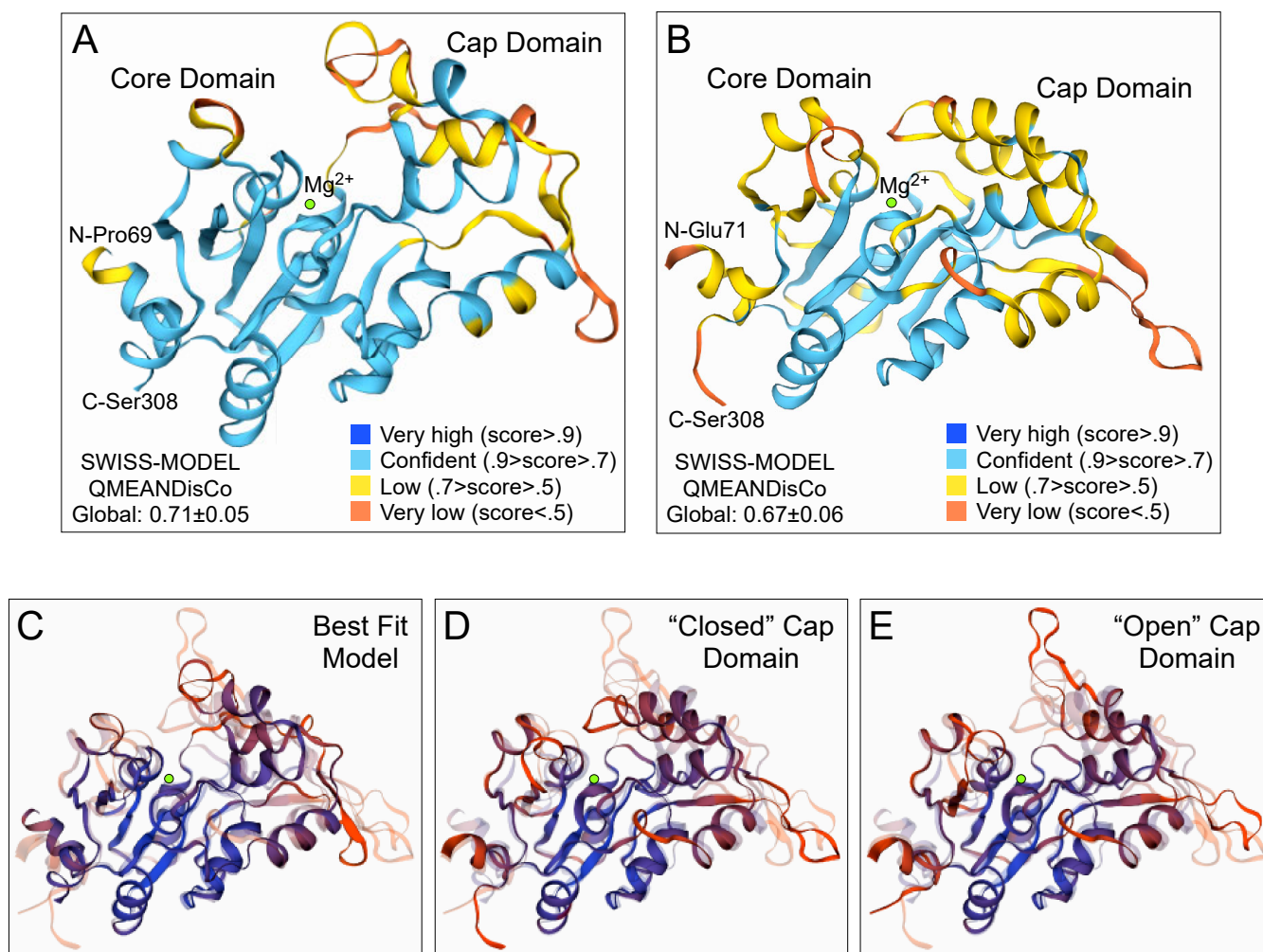


Figure 6. Homology models of the three-dimensional structure of the GPD2 GPP domain generated in automated mode with Swiss-Model. (A) Model constructed based on the crystal structure of *D. salina* dsGPDH 6iuy.1.a, shown in cartoon representation and colored according to confidence class. The green sphere corresponds to a Mg²⁺ atom. (B) Model constructed based on the crystal structure of human phosphoserine phosphatase 6hyj.1.A. (C–E) For comparison purposes, model superposition is shown in cartoon representation and colored according to confidence gradient (blue = high confidence --> orange = low confidence). The green sphere corresponds to a Mg²⁺ atom. (C) Full color saturation model based on *D. salina* dsGPDH 6iuy.1.a. (D) Full color saturation model based on human phosphoserine phosphatase 6hyj.1.A. (E) Full color saturation model based on human phosphoserine phosphatase 6hyj.2.A.

4. Discussion

Many chlorophytes accumulate intracellular glycerol, as a compatible solute, under high salinity [1,2,5,6,12–17,66]. Although a freshwater alga, *C. reinhardtii* cell division is strongly inhibited only at 200 mM NaCl, which corresponds to approximately 40% of seawater

ter salinity [13,67]. Chloroplast-localized bidomain GPD enzymes, consisting of canonical glycerol-3-phosphate dehydrogenase domains fused with an N-terminal phosphoserine phosphatase-like domain, have been implicated in the response to salt stress [5,15,17,18]. In *C. reinhardtii*, transcriptomic and RNA interference analyses also support a role for these enzymes in triacylglycerol accumulation under nitrogen or phosphorus deprivation [15,20,27,28]. However, the regulation of these bidomain GPDs under different environmental stresses is not clearly understood. As proposed before [15], for membrane glycerolipid and TAG synthesis under normal or nutrient-deprived conditions, the production of G3P catalyzed solely by the canonical GPD domains would be energetically favored. On the other hand, under osmotic/salinity stress, the synthesis of glycerol would also require an active G3P phosphatase domain.

The canonical GPD domains from several *Dunaliella* bidomain enzymes have been reported to be active in diverse contexts: in in vitro assays with purified recombinant proteins [17,25], in the complementation of yeast GPD deletion mutants [25], and in tests with the partly purified, by DEAE cellulose chromatography, endogenous osmoregulated enzyme [68]. The latter was also the case when the enzyme was purified from cells grown at low NaCl concentration [68], which accumulate very little glycerol [12,46]. Likewise, *C. reinhardtii* bidomain GPD enzymes have been reported to display glycerol-3-phosphate dehydrogenase activity in the complementation of yeast deletion mutants [19,20] and in in vitro assays with recombinant proteins [15]. In addition, *C. reinhardtii* GPD2 overexpression strains, grown in nutrient replete TAP medium, showed a significant increase in diglycerides (but not glycerol) relative to the wild type [20], as expected if transgenic GPD2 mostly synthesizes G3P under normal environmental conditions. Based on these observations, we favor the hypothesis that the canonical GPD domains of the chloroplast-localized bidomain enzymes are active in vivo under (nearly) all environmental conditions. Additionally, in the experiments reported here, the stability of transgenic GPD2 protein was very similar in cells cultured in nutrient replete medium as in those subject to nitrogen deprivation for 48 h (Figure 3C), possibly suggesting a similar enzyme conformation under these conditions, where mainly G3P synthesis is expected. However, in several algal species, transcriptional (and potentially translational) regulation may constrain endogenous bidomain GPD protein expression only to cells subject to certain environmental stresses [5,15,18–20,24,25,27,28].

In contrast, conflicting results have been published on the G3P phosphatase activity of bidomain GPD enzymes. An ~86 kDa protein (likely a bidomain GPD enzyme), partly purified from *D. salina*, showed unstable G3P phosphatase activity [69]. In addition, its K_m for G3P, about 2.7 mM, was considered unusually high [68,69]. Using purified recombinant proteins in in vitro assays, no G3P phosphatase activity was detected for two *D. viridis* bidomain GPD enzymes [25]. However, recombinant *C. reinhardtii* GPD2 and *D. salina* osmoregulated GPDH were able to convert DHAP directly to glycerol in biochemical assays [15,17]. Mutation of key aspartate residues in the phosphoserine phosphatase-like domain of GPD2 abolished its G3P phosphatase activity, substantiating its function as a GPP [15]. In the present work with overexpression strains, transgenic GPD2 protein was clearly detected and fairly stable in cells grown photoautotrophically in minimal medium (Figure 3A), but no glycerol accumulation was detected under these conditions (Figure 3B). These observations suggested that GPP domain activity might be context dependent and possibly regulated at the post-translational level.

Interestingly, the *C. reinhardtii* GPD2 gene was significantly upregulated upon exposure of cells to NaCl ([15,19,20], this work) but, in several proteomic experiments examining cells under osmotic/salt stress, the GPD2 protein was not detected [16,23]. Likewise, genes encoding certain bidomain GPD enzymes were transcriptionally induced in *Dunaliella* spp. exposed to hypersalinity [18,24,25] but, at least in *D. tertiolecta* [26] and *D. salina* [70], no changes were detected in the abundance of the corresponding proteins. In this study, we observed that the stability of the transgenic GPD2 protein was greatly reduced when cells were cultured in HS medium containing NaCl (Figures 3A and S1). Yet, under these condi-

tions, OX-12 cells (unlike the wild type) were able to accumulate glycerol in the absence of de novo cytoplasmic protein synthesis blocked by the addition of cycloheximide (Figure 3B). Thus, pre-existing transgenic GPD2 protein (and likely also endogenous bidomain GPDs) appears to be altered by NaCl stress; and its destabilization may be related to activation (or de-repression) of the GPP domain allowing glycerol synthesis (please see below).

We used several approaches, mostly relying on pharmacological treatments, to explore the mechanism(s) involved in the proposed post-translational GPP domain regulation under salinity stress. However, the ROS scavenger N-acetyl-L-cysteine, the protein phosphatase inhibitor okadaic acid, and the TOR kinase inhibitor Torin1 did not affect glycerol accumulation by transgenic GPD2 strains upon salinity stress (Figure 4 and Figure S2C). Only staurosporine, a non-specific protein kinase inhibitor, was able to prevent the NaCl-induced synthesis of glycerol by pre-existing transgenic GPD2 (Figure 5D). Intriguingly, we still observed GPD2 protein destabilization under these conditions (Figure 5C). Proteomic experiments enriching AcV5-tagged GPD2 protein by affinity purification, followed by identification of differentially phosphorylated peptides by LC-MS/MS only detected Ser145 (within the GPD2 GPP domain) as potentially phosphorylated upon NaCl stress (Figure S3A). While this residue is within a conserved motif in bidomain GPDs from diverse microalgae (Figure S3B), it remains uncertain whether its phosphorylation is functionally relevant. Moreover, the corresponding peptide was only identified at low/medium confidence due to its low abundance. However, in cells grown photoheterotrophically in TAP medium under normal conditions, the same peptide has been reported to be unphosphorylated [71]. Additionally, we cannot rule out that a kinase(s) inhibited by staurosporine might modify another protein which, in turn, affects GPD2 activity. Nevertheless, our results, taken together, strongly indicate that the GPD2 protein is post-translationally regulated upon NaCl stress.

Post-translational regulation of enzymes involved in osmotic/salt stress responses is supported by evidence in various organisms [6,11,14,21,72]. In *D. salina*, de novo protein synthesis was not required for the osmotic response, and the increase in glycerol content triggered by exposure to high salinity [72]. In *Phycomyces blakesleeanus*, a G3P phosphatase has been proposed to be activated by phosphorylation mediated by a cyclic-AMP-dependent protein kinase [73]. Moreover, in *C. reinhardtii*, metabolome analysis revealed that the proline-biosynthetic pathway is strongly induced upon salt stress but, in parallel proteomic analyses, enzymes in this pathway did not change in abundance [21]. Other studies also reported very rapid metabolic changes and remodeling of primary metabolism in *C. reinhardtii* when exposed to osmotic stress [16]. These observations suggest that initial responses to osmotic/salinity stress may involve the post-translational regulation of existing enzymes, allowing cells to adjust rapidly their metabolism to cope with the stress. MAPKs and other protein kinases have been characterized as components of signaling pathways implicated in osmotic/salt stress tolerance in diverse organisms, including microalgae [11,16,51,52]. Phosphorylation is also a common mechanism to modulate protein function in chloroplasts [74,75] and, based on the results of the staurosporine treatments, a protein kinase(s) is apparently involved in the post-translational regulation of plastid-localized GPD2.

Based on structural modeling analyses of the GPD2 GPP domain (Figure 6), some tentative hypotheses can be proposed regarding the observed changes in GPD2 protein stability and activity under hypersalinity conditions. Assuming, as previously argued [15,17], that GPP catalysis in bidomain GPDs is similar to that of phosphoserine phosphatases [42,65], it is tempting to speculate that an active GPP domain will undergo dynamic switching between open and closed conformations of its cap domain. The somewhat unfolded conformation in the open state would likely make the GPD2 protein more prone to protease degradation, explaining its reduced stability under salinity stress. The initial change in GPD2 conformation, from a supposedly inactive compactly folded GPP domain, could possibly be triggered by alterations in the intracellular milieu when cells are exposed to higher osmolarity/salinity, such as changes in pH, ionic composition, or molecular crowd-

ing. Certainly, this appears to happen, at least in certain contexts, in recombinant bidomain GPDs with demonstrated phosphatase activity in *in vitro* assays. A recombinant enzyme locked in a partly open conformation of the cap domain would presumably be able to function, but not at full enzymatic capacity. However, *in vivo*, dynamic switching between open and closed states might be required for efficient multiple-turnover catalysis and rapid glycerol synthesis. This dynamic switching could possibly be inhibited by staurosporine but, if so, the mechanism(s) remains uncertain. In summary, our results suggest that the GPP domain of bidomain GPD enzymes is activated post-translationally upon salinity stress and a protein kinase may be involved in this process, but extensive additional work will be needed to characterize the actual mechanism(s).

5. Conclusions

Some microalgae are remarkable in their ability to thrive under a wide range of salinity conditions, which involves, among other responses [6,66], the capacity to rapidly adjust their intracellular concentration of compatible solutes such as glycerol. As a probable adaptation to fluctuating osmolarity/salinity in their habitats, core chlorophytes have evolved unusual, chloroplast-localized bidomain GPDs capable of converting DHAP directly to glycerol. These enzymes possess canonical glycerol-3-phosphate dehydrogenase domains fused to a glycerol-3-phosphate phosphatase domain, and have been implicated in both glycerol and TAG synthesis. It is also becoming apparent that the expression and activity of these enzymes are tightly regulated at multiple levels. Extensive evidence suggests that the corresponding genes are transcriptionally controlled, and the work reported here supports the existence, at least for *C. reinhardtii* GPD2, of intricate post-translational regulation. Indeed, the GPP domain of GPD2 appears to be activated, via a mechanism(s) involving a protein kinase(s), only upon exposure of cells to salt stress. Elucidating the molecular basis of these mechanisms may provide insights into the fast acclimation responses of microalgae to osmotic/salinity stress, but it may also have biotechnological implications. Pagliaro [76] proposed that glycerol may become one of the key platform compounds for the synthesis of biopolymers and other high-value chemicals in the upcoming bioeconomy. Microalgae are being studied as biofactories for glycerol production by direct CO₂ capture, and the introduction of bidomain GPDs into yeasts has been suggested as another way to improve glycerol bioproduction [26,67,77]. However, successful metabolic engineering for glycerol production employing bidomain GPDs, in either homologous or heterologous hosts, will likely require a greater understanding of their regulatory controls.

Supplementary Materials: The following supporting information can be downloaded at: <https://www.mdpi.com/article/10.3390/phycology4020012/s1>, Figure S1. Analysis of GPD2 protein abundance in overexpression strains OX-9, OX-29, and OX-30; Figure S2. Effect of light and the ROS scavenger *N*-acetyl-L-cysteine (NAC) on glycerol accumulation by the wild type and OX-12 strains; Figure S3. Phosphorylation of the GPP domain of GPD2 in OX-12 cells exposed to salinity stress.

Author Contributions: Conceptualization: D.M.-S. and H.C.; Investigation: I.C.-P., B.S., Y.K. and D.M.-S.; Data Analyses: I.C.-P., B.S., Y.K., D.M.-S. and H.C.; Writing—Original Draft Preparation: I.C.-P. and H.C.; Writing—Review and Editing: I.C.-P., B.S., Y.K., D.M.-S. and H.C. All authors have read and agreed to the published version of the manuscript.

Funding: This work was supported in part by a grant from the National Science Foundation (NSF) to H.C. (award number 2131783).

Institutional Review Board Statement: Not applicable.

Informed Consent Statement: Not applicable.

Data Availability Statement: Any further data related to this study are available on request from the corresponding author.

Conflicts of Interest: The authors declare no conflicts of interest.

References

1. Ahmad, I.; Hellebust, J.A. The Role of Glycerol and Inorganic Ions in Osmoregulatory Responses of the Euryhaline Flagellate *Chlamydomonas pulsatilla* Wollenweber. *Plant Physiol.* **1986**, *82*, 406–410. [[CrossRef](#)]
2. Miyasaka, H.; Ohnishi, Y.; Akano, T.; Fukatsu, K.; Mizoguchi, T.; Yagi, K.; Maeda, I.; Ikuta, Y.; Matsumoto, H.; Shioji, N.; et al. Excretion of Glycerol by the Marine *Chlamydomonas* sp. Strain W-80 in High CO₂ Cultures. *J. Ferment. Bioeng.* **1998**, *85*, 122–124. [[CrossRef](#)]
3. Sasso, S.; Stibor, H.; Mittag, M.; Grossman, A.R. From molecular manipulation of domesticated *Chlamydomonas reinhardtii* to survival in nature. *eLife* **2018**, *7*, e39233. [[CrossRef](#)]
4. Salomé, P.A.; Merchant, S.S. A Series of Fortunate Events: Introducing *Chlamydomonas* as a Reference Organism. *Plant Cell* **2019**, *31*, 1682–1707. [[CrossRef](#)] [[PubMed](#)]
5. Raymond, J.A.; Morgan-Kiss, R.; Stahl-Rommel, S. Glycerol Is an Osmoprotectant in Two Antarctic *Chlamydomonas* Species from an Ice-Covered Saline Lake and Is Synthesized by an Unusual Bidomain Enzyme. *Front. Plant Sci.* **2020**, *11*, 1259. [[CrossRef](#)] [[PubMed](#)]
6. Bazzani, E.; Lauritano, C.; Mangoni, O.; Bolinesi, F.; Saggiomo, M. *Chlamydomonas* Responses to Salinity Stress and Possible Biotechnological Exploitation. *J. Mar. Sci. Eng.* **2021**, *9*, 1242. [[CrossRef](#)]
7. Pröschold, T.; Marin, B.; Schlösser, U.G.; Melkonian, M. Molecular Phylogeny and Taxonomic Revision of *Chlamydomonas* (Chlorophyta). I. Emendation of *Chlamydomonas* Ehrenberg and *Chloromonas* Gobi, and Description of *Oogamochlamys* gen. nov. and *Lobochlamys* gen. nov. *Protist* **2001**, *152*, 265–300. [[CrossRef](#)]
8. Craig, R.J.; Hasan, A.R.; Ness, R.W.; Keightley, P.D. Comparative genomics of *Chlamydomonas*. *Plant Cell* **2021**, *33*, 1016–1041. [[CrossRef](#)]
9. Merchant, S.S.; Prochnik, S.E.; Vallon, O.; Harris, E.H.; Karpowicz, S.J.; Witman, G.B.; Terry, A.; Salamov, A.; Fritz-Laylin, L.K.; Maréchal-Drouard, L.; et al. The *Chlamydomonas* Genome Reveals the Evolution of Key Animal and Plant Functions. *Science* **2007**, *318*, 245–250. [[CrossRef](#)]
10. Oren, A. Glycerol metabolism in hypersaline environments. *Environ. Microbiol.* **2017**, *19*, 851–863. [[CrossRef](#)]
11. Blomberg, A. Yeast osmoregulation—glycerol still in pole position. *FEMS Yeast Res.* **2022**, *22*, foac035. [[CrossRef](#)]
12. Ben-Amotz, A.; Avron, M. The Role of Glycerol in the Osmotic Regulation of the Halophitic Alga *Dunaliella parva*. *Plant Physiol.* **1973**, *51*, 875–878. [[CrossRef](#)]
13. León, R.; Galván, F. Halotolerance Studies on *Chlamydomonas reinhardtii*: Glycerol Excretion by Free and Immobilized Cells. *J. Appl. Phycol.* **1994**, *6*, 13–20. [[CrossRef](#)]
14. Chen, H.; Jiang, J.G. Osmotic responses of *Dunaliella* to the changes of salinity. *J. Cell. Physiol.* **2009**, *219*, 251–258. [[CrossRef](#)] [[PubMed](#)]
15. Morales-Sánchez, D.; Kim, Y.; Terng, E.L.; Peterson, L.; Cerutti, H. A Multidomain Enzyme, with Glycerol-3-Phosphate Dehydrogenase and Phosphatase Activities, Is Involved in a Chloroplastic Pathway for Glycerol Synthesis in *Chlamydomonas reinhardtii*. *Plant. J.* **2017**, *90*, 1079–1092. [[CrossRef](#)] [[PubMed](#)]
16. Colina, F.J.; Carbó, M.; Cañal, M.J.; Valledor, L. A complex metabolic rearrangement towards the accumulation of glycerol and sugars consequence of a proteome remodeling is required for the survival of *Chlamydomonas reinhardtii* growing under osmotic stress. *Environ. Exp. Bot.* **2020**, *180*, 104261. [[CrossRef](#)]
17. He, Q.; Toh, J.D.; Ero, R.; Qiao, Z.; Kumar, V.; Serra, A.; Tan, J.; Sze, S.K.; Gao, Y.G. The unusual di-domain structure of *Dunaliella salina* glycerol-3-phosphate dehydrogenase enables direct conversion of dihydroxyacetone phosphate to glycerol. *Plant J.* **2020**, *102*, 153–164. [[CrossRef](#)] [[PubMed](#)]
18. Wu, Q.; Lan, Y.; Cao, X.; Yao, H.; Qiao, D.; Xu, H.; Cao, Y. Characterization and diverse evolution patterns of glycerol-3-phosphate dehydrogenase family genes in *Dunaliella salina*. *Gene* **2019**, *710*, 161–169. [[CrossRef](#)]
19. Casais-Molina, M.L.; Peraza-Echeverría, S.; Echevarría-Machado, I.; Herrera-Valencia, V.A. Expression of *Chlamydomonas reinhardtii* CrGPDH2 and CrGPDH3 cDNAs in Yeast Reveals That They Encode Functional Glycerol-3-Phosphate Dehydrogenases Involved in Glycerol Production and Osmotic Stress Tolerance. *J. Appl. Phycol.* **2016**, *28*, 219–226. [[CrossRef](#)]
20. Driver, T.; Trivedi, D.K.; McIntosh, O.A.; Dean, A.P.; Goodacre, R.; Pittman, J.K. Two Glycerol-3-Phosphate Dehydrogenases from *Chlamydomonas* Have Distinct Roles in Lipid Metabolism. *Plant Physiol.* **2017**, *174*, 2083–2097. [[CrossRef](#)]
21. Mastrobuoni, G.; Irgang, S.; Pietzke, M.; Aßmus, H.E.; Wenzel, M.; Schulze, W.X.; Kempa, S. Proteome Dynamics and Early Salt Stress Response of the Photosynthetic Organism *Chlamydomonas reinhardtii*. *BMC Genom.* **2012**, *13*, 215. [[CrossRef](#)] [[PubMed](#)]
22. Tietel, Z.; Wikoff, W.R.; Kind, T.; Fiehn, O. Hyperosmotic stress in *Chlamydomonas* induces metabolomic changes in biosynthesis of complex lipids. *Eur. J. Phycol.* **2020**, *55*, 11–29. [[CrossRef](#)]
23. Yokthongwattana, C.; Mahong, B.; Roytrakul, S.; Phaonaklop, N.; Narangajavana, J.; Yokthongwattana, K. Proteomic Analysis of Salinity-Stressed *Chlamydomonas reinhardtii* Revealed Differential Suppression and Induction of a Large Number of Important Housekeeping Proteins. *Planta* **2012**, *235*, 649–659. [[CrossRef](#)] [[PubMed](#)]
24. He, Q.; Lin, Y.; Tan, H.; Zhou, Y.; Wen, Y.; Gan, J.; Li, R.; Zhang, Q. Transcriptomic profiles of *Dunaliella salina* in response to hypersaline stress. *BMC Genom.* **2020**, *21*, 115. [[CrossRef](#)]

25. He, Y.; Meng, X.; Fan, Q.; Sun, X.; Xu, Z.; Song, R. Cloning and characterization of two novel chloroplastic glycerol-3-phosphate dehydrogenases from *Dunaliella viridis*. *Plant Mol. Biol.* **2009**, *71*, 193–205. [[CrossRef](#)] [[PubMed](#)]
26. Keil, L.; Mehler, N.; Cavelius, P.; Garbe, D.; Haack, M.; Ritz, M.; Awad, D.; Brück, T. The Time-Resolved Salt Stress Response of *Dunaliella tertiolecta*—A Comprehensive System Biology Perspective. *Int. J. Mol. Sci.* **2023**, *24*, 15374. [[CrossRef](#)] [[PubMed](#)]
27. Goodenough, U.; Blaby, I.; Casero, D.; Gallaher, S.D.; Goodson, C.; Johnson, S.; Lee, J.H.; Merchant, S.S.; Pellegrini, M.; Roth, R.; et al. The path to triacylglyceride obesity in the *sta6* strain of *Chlamydomonas reinhardtii*. *Eukaryot. Cell* **2014**, *13*, 591–613. [[CrossRef](#)] [[PubMed](#)]
28. Schmollinger, S.; Mühlhaus, T.; Boyle, N.R.; Blaby, I.K.; Casero, D.; Mettler, T.; Moseley, J.L.; Kropat, J.; Sommer, F.; Strenkert, D.; et al. Nitrogen-Sparing Mechanisms in *Chlamydomonas* Affect the Transcriptome, the Proteome, and Photosynthetic Metabolism. *Plant Cell* **2014**, *26*, 1410–1435. [[CrossRef](#)]
29. Johnson, X.; Alric, J. Central carbon metabolism and electron transport in *Chlamydomonas reinhardtii*: Metabolic constraints for carbon partitioning between oil and starch. *Eukaryot. Cell* **2013**, *12*, 776–793. [[CrossRef](#)]
30. Msanne, J.; Xu, D.; Konda, A.R.; Casas-Mollano, J.A.; Awada, T.; Cahoon, E.B.; Cerutti, H. Metabolic and gene expression changes triggered by nitrogen deprivation in the photoautotrophically grown microalgae *Chlamydomonas reinhardtii* and *Coccomyxa* sp. C-169. *Phytochemistry* **2012**, *75*, 50–59. [[CrossRef](#)]
31. Sueoka, N. Mitotic replication of deoxyribonucleic acid in *Chlamydomonas reinhardtii*. *Proc. Natl. Acad. Sci. USA* **1960**, *46*, 83–91. [[CrossRef](#)] [[PubMed](#)]
32. Harris, E.H. *The Chlamydomonas Sourcebook: A Comprehensive Guide to Biology and Laboratory Use*; Academic Press: San Diego, CA, USA, 1989.
33. Lawrence, S.D.; Novak, N.G.; Slack, J.M. Epitope tagging: A monoclonal antibody specific for recombinant fusion proteins in plants. *Biotechniques* **2003**, *35*, 488–492. [[CrossRef](#)] [[PubMed](#)]
34. Fischer, N.; Rochaix, J.D. The flanking regions of *PsaD* drive efficient gene expression in the nucleus of the green alga *Chlamydomonas reinhardtii*. *Mol. Genet. Genom.* **2001**, *265*, 888–894. [[CrossRef](#)] [[PubMed](#)]
35. Stevens, D.R.; Rochaix, J.D.; Purton, S. The bacterial phleomycin resistance gene *ble* as a dominant selectable marker in *Chlamydomonas*. *Mol. Gen. Genet.* **1996**, *251*, 23–30. [[PubMed](#)]
36. Plucinak, T.M.; Horken, K.M.; Jiang, W.; Fostvedt, J.; Nguyen, S.T.; Weeks, D.P. Improved and versatile viral 2A platforms for dependable and inducible high-level expression of dicistronic nuclear genes in *Chlamydomonas reinhardtii*. *Plant J.* **2015**, *82*, 717–729. [[CrossRef](#)] [[PubMed](#)]
37. Kim, Y.; Terng, E.L.; Riekhof, W.R.; Cahoon, E.B.; Cerutti, H. Endoplasmic reticulum acyltransferase with prokaryotic substrate preference contributes to triacylglycerol assembly in *Chlamydomonas*. *Proc. Natl. Acad. Sci. USA* **2018**, *115*, 1652–1657. [[CrossRef](#)] [[PubMed](#)]
38. Sambrook, J.; Russell, D.W. *Molecular Cloning—A Laboratory Manual*; Cold Spring Harbor Laboratory Press: Cold Spring Harbor, NY, USA, 2001.
39. Ma, X.; Ibrahim, F.; Kim, E.J.; Shaver, S.; Becker, J.; Razvi, F.; Cerny, R.L.; Cerutti, H. An ortholog of the Vasa intronic gene is required for small RNA-mediated translation repression in *Chlamydomonas reinhardtii*. *Proc. Natl. Acad. Sci. USA* **2020**, *117*, 761–770. [[CrossRef](#)] [[PubMed](#)]
40. Zogli, P.; Alvarez, S.; Naldrett, M.J.; Palmer, N.A.; Koch, K.G.; Pingault, L.; Bradshaw, J.D.; Twigg, P.; Heng-Moss, T.M.; Louis, J.; et al. Greenbug (*Schizaphis graminum*) herbivory significantly impacts protein and phosphorylation abundance in switchgrass (*Panicum virgatum*). *Sci. Rep.* **2020**, *10*, 14842. [[CrossRef](#)]
41. Waterhouse, A.; Bertoni, M.; Bienert, S.; Studer, G.; Tauriello, G.; Gumienny, R.; Heer, F.T.; de Beer, T.A.P.; Rempfer, C.; Bordoli, L.; et al. SWISS-MODEL: Homology modelling of protein structures and complexes. *Nucleic Acids Res.* **2018**, *46*, W296–W303. [[CrossRef](#)]
42. Haufroid, M.; Mirgaux, M.; Leherte, L.; Wouters, J. Crystal structures and snapshots along the reaction pathway of human phosphoserine phosphatase. *Acta Crystallogr. D Struct. Biol.* **2019**, *75*, 592–604. [[CrossRef](#)]
43. Jumper, J.; Evans, R.; Pritzel, A.; Green, T.; Figurnov, M.; Ronneberger, O.; Tunyasuvunakool, K.; Bates, R.; Židek, A.; Potapenko, A.; et al. Highly accurate protein structure prediction with AlphaFold. *Nature* **2021**, *596*, 583–589. [[CrossRef](#)] [[PubMed](#)]
44. RStudio Team. *RStudio: Integrated Development Environment for R*. RStudio; PBC: Boston, MA, USA, 2021; Available online: <http://www.rstudio.com/> (accessed on 15 December 2023).
45. Ma, X.; Kim, E.J.; Kook, I.; Ma, F.; Voshall, A.; Moriyama, E.; Cerutti, H. Small interfering RNA-mediated translation repression alters ribosome sensitivity to inhibition by cycloheximide in *Chlamydomonas reinhardtii*. *Plant Cell* **2013**, *25*, 985–998. [[CrossRef](#)] [[PubMed](#)]
46. Goyal, A. Osmoregulation in *Dunaliella*, Part II: Photosynthesis and starch contribute carbon for glycerol synthesis during a salt stress in *Dunaliella tertiolecta*. *Plant Physiol. Biochem.* **2007**, *45*, 705–710. [[CrossRef](#)] [[PubMed](#)]
47. Davis, R.W.; Carvalho, B.J.; Jones, H.D.; Singh, S. The role of photo-osmotic adaptation in semi-continuous culture and lipid particle release from *Dunaliella viridis*. *J. Appl. Phycol.* **2015**, *27*, 109–123. [[CrossRef](#)] [[PubMed](#)]
48. Sun, S.Y. N-acetylcysteine, reactive oxygen species and beyond. *Cancer Biol. Ther.* **2010**, *9*, 109–110. [[CrossRef](#)] [[PubMed](#)]
49. Voigt, J.; Woestemeyer, J. Protease Inhibitors Cause Necrotic Cell Death in *Chlamydomonas reinhardtii* by Inducing the Generation of Reactive Oxygen Species. *J. Eukaryot. Microbiol.* **2015**, *62*, 711–721. [[CrossRef](#)] [[PubMed](#)]

50. Pérez-Pérez, M.E.; Lemaire, S.D.; Crespo, J.L. Control of Autophagy in *Chlamydomonas* Is Mediated through Redox-Dependent Inactivation of the ATG4 Protease. *Plant Physiol.* **2016**, *172*, 2219–2234. [[CrossRef](#)] [[PubMed](#)]
51. Zhao, R.; Ng, D.H.P.; Fang, L.; Chow, Y.Y.S.; Lee, Y.K. MAPK in *Dunaliella tertiolecta* regulates glycerol production in response to osmotic shock. *Eur. J. Phycol.* **2016**, *51*, 119–128. [[CrossRef](#)]
52. Tang, Z.; Cao, X.; Zhang, Y.; Jiang, J.; Qiao, D.; Xu, H.; Cao, Y. Two splice variants of the DsMEK1 mitogen-activated protein kinase kinase (MAPKK) are involved in salt stress regulation in *Dunaliella salina* in different ways. *Biotechnol. Biofuels* **2020**, *13*, 147. [[CrossRef](#)]
53. Dounay, A.B.; Forsyth, C.J. Okadaic acid: The archetypal serine/threonine protein phosphatase inhibitor. *Curr. Med. Chem.* **2002**, *9*, 1939–1980. [[CrossRef](#)]
54. Valdiglesias, V.; Prego-Faraldo, M.V.; Pásaro, E.; Méndez, J.; Laffon, B. Okadaic acid: More than a diarrhetic toxin. *Mar. Drugs* **2013**, *11*, 4328–4349. [[CrossRef](#)] [[PubMed](#)]
55. Liang, Y.; Zhu, X.; Wu, Q.; Pan, J. Ciliary Length Sensing Regulates IFT Entry via Changes in FLA8/KIF3B Phosphorylation to Control Ciliary Assembly. *Curr. Biol.* **2018**, *28*, 2429–2435. [[CrossRef](#)] [[PubMed](#)]
56. Lin, H.; Miller, M.L.; Granas, D.M.; Dutcher, S.K. Whole genome sequencing identifies a deletion in protein phosphatase 2A that affects its stability and localization in *Chlamydomonas reinhardtii*. *PLoS Genet.* **2013**, *9*, e1003841. [[CrossRef](#)] [[PubMed](#)]
57. Werth, E.G.; McConnell, E.W.; Couso Lianez, I.; Perrine, Z.; Crespo, J.L.; Umen, J.G.; Hicks, L.M. Investigating the effect of target of rapamycin kinase inhibition on the *Chlamydomonas reinhardtii* phosphoproteome: From known homologs to new targets. *New Phytol.* **2019**, *221*, 247–260. [[CrossRef](#)] [[PubMed](#)]
58. Henriques, R.; Calderan-Rodrigues, M.J.; Crespo, J.L.; Baena-González, E.; Caldana, C. Growing of the TOR world. *J. Exp. Bot.* **2022**, *73*, 6987–6992. [[CrossRef](#)] [[PubMed](#)]
59. Deprost, D.; Yao, L.; Sormani, R.; Moreau, M.; Leterreux, G.; Nicolai, M.; Bedu, M.; Robaglia, C.; Meyer, C. The *Arabidopsis* TOR kinase links plant growth, yield, stress resistance and mRNA translation. *EMBO Rep.* **2007**, *8*, 864–870. [[CrossRef](#)] [[PubMed](#)]
60. Pereyra, C.M.; Aznar, N.R.; Rodriguez, M.S.; Salerno, G.L.; Martínez-Noël, G.M.A. Target of rapamycin signaling is tightly and differently regulated in the plant response under distinct abiotic stresses. *Planta* **2019**, *251*, 21. [[CrossRef](#)]
61. Bakshi, A.; Moin, M.; Madhav, M.S.; Datla, R.; Kirti, P.B. Target of Rapamycin (TOR) negatively regulates chlorophyll degradation and lipid peroxidation and controls responses under abiotic stress in *Arabidopsis thaliana*. *Plant Stress* **2021**, *2*, 100020. [[CrossRef](#)]
62. Couso, I.; Pérez-Pérez, M.E.; Ford, M.M.; Martínez-Force, E.; Hicks, L.M.; Umen, J.G.; Crespo, J.L. Phosphorus Availability Regulates TORC1 Signaling via LST8 in *Chlamydomonas*. *Plant Cell* **2020**, *32*, 69–80. [[CrossRef](#)]
63. Karaman, M.W.; Herrgard, S.; Treiber, D.K.; Gallant, P.; Atteridge, C.E.; Campbell, B.T.; Chan, K.W.; Ciceri, P.; Davis, M.I.; Edeen, P.T.; et al. A quantitative analysis of kinase inhibitor selectivity. *Nat. Biotechnol.* **2008**, *26*, 127–132. [[CrossRef](#)]
64. Schmollinger, S.; Schulz-Raffelt, M.; Strenkert, D.; Veyel, D.; Vallon, O.; Schroda, M. Dissecting the heat stress response in *Chlamydomonas* by pharmaceutical and RNAi approaches reveals conserved and novel aspects. *Mol. Plant.* **2013**, *6*, 1795–1813. [[CrossRef](#)] [[PubMed](#)]
65. Wang, W.; Cho, H.S.; Kim, R.; Jancarik, J.; Yokota, H.; Nguyen, H.H.; Grigoriev, I.V.; Wemmer, D.E.; Kim, S.H. Structural characterization of the reaction pathway in phosphoserine phosphatase: Crystallographic “snapshots” of intermediate states. *J. Mol. Biol.* **2002**, *319*, 421–431. [[CrossRef](#)] [[PubMed](#)]
66. Shetty, P.; Gitau, M.M.; Maróti, G. Salinity Stress Responses and Adaptation Mechanisms in Eukaryotic Green Microalgae. *Cells* **2019**, *8*, 1657. [[CrossRef](#)] [[PubMed](#)]
67. Demmig-Adams, B.; Burch, T.A.; Stewart, J.J.; Savage, E.L.; Adams III, W.W. Algal glycerol accumulation and release as a sink for photosynthetic electron transport. *Algal Res.* **2017**, *21*, 161–168. [[CrossRef](#)]
68. Gee, R.; Goyal, A.; Byerrum, R.U.; Tolbert, N.E. Two Isoforms of Dihydroxyacetone Phosphate Reductase from the Chloroplasts of *Dunaliella tertiolecta*. *Plant Physiol.* **1993**, *103*, 243–249. [[CrossRef](#)] [[PubMed](#)]
69. Sussman, I.; Avron, M. Characterization and partial purification of DL-glycerol-1-phosphatase from *Dunaliella salina*. *Biochim. Biophys. Acta* **1981**, *661*, 199–204. [[CrossRef](#)]
70. Wang, Y.; Cong, Y.; Wang, Y.; Guo, Z.; Yue, J.; Xing, Z.; Gao, X.; Chai, X. Identification of Early Salinity Stress-Responsive Proteins in *Dunaliella salina* by isobaric tags for relative and absolute quantitation (iTRAQ)-Based Quantitative Proteomic Analysis. *Int. J. Mol. Sci.* **2019**, *20*, 599. [[CrossRef](#)] [[PubMed](#)]
71. McConnell, E.W.; Werth, E.G.; Hicks, L.M. The phosphorylated redox proteome of *Chlamydomonas reinhardtii*: Revealing novel means for regulation of protein structure and function. *Redox Biol.* **2018**, *17*, 35–46. [[CrossRef](#)]
72. Sadka, A.; Lers, A.; Zamir, A.; Avron, M. A critical examination of the role of de novo protein synthesis in the osmotic adaptation of the halotolerant alga *Dunaliella*. *FEBS Lett.* **1989**, *244*, 93–98. [[CrossRef](#)]
73. van Schaftingen, E.; van Laere, A.J. Glycerol formation after the breaking of dormancy of *Phycomyces blakesleeanus* spores. Role of an interconvertible glycerol-3-phosphatase. *Eur. J. Biochem.* **1985**, *148*, 399–404. [[CrossRef](#)]
74. Bayer, R.G.; Stael, S.; Rocha, A.G.; Mair, A.; Vothknecht, U.C.; Teige, M. Chloroplast-localized protein kinases: A step forward towards a complete inventory. *J. Exp. Bot.* **2012**, *63*, 1713–1723. [[CrossRef](#)] [[PubMed](#)]
75. White-Gloria, C.; Johnson, J.J.; Marritt, K.; Kataya, A.; Vahab, A.; Moorhead, G.B. Protein Kinases and Phosphatases of the Plastid and Their Potential Role in Starch Metabolism. *Front. Plant Sci.* **2018**, *9*, 1032. [[CrossRef](#)] [[PubMed](#)]

-
76. Pagliaro, M. Glycerol: A key platform chemical of the forthcoming bioeconomy. In *Glycerol: The Renewable Platform Chemical*; Pagliaro, M., Ed.; Elsevier: Amsterdam, The Netherlands, 2017; pp. 109–132.
 77. Semkiv, M.V.; Ruchala, J.; Dmytruk, K.V.; Sibirny, A.A. 100 Years Later, What Is New in Glycerol Bioproduction? *Trends Biotechnol.* **2020**, *38*, 907–916. [[CrossRef](#)] [[PubMed](#)]

Disclaimer/Publisher’s Note: The statements, opinions and data contained in all publications are solely those of the individual author(s) and contributor(s) and not of MDPI and/or the editor(s). MDPI and/or the editor(s) disclaim responsibility for any injury to people or property resulting from any ideas, methods, instructions or products referred to in the content.